Single-Particle Dynamics

Yannis PAPAPHILIPPOU

June 5, 2001

Outline

- The single-particle relativistic Hamiltonian
- Linear betatron motion and action-angle variables
- Generalized non-linear Hamiltonian
- Classical perturbation theory
  - Canonical perturbation method
  - Application to the accelerator Hamiltonian
  - Resonance driving terms and tune-shift
- The single resonance treatment
  - “Secular” perturbation theory and resonance overlap criterion
  - Application to the accelerator Hamiltonian - Resonance widths

Outline (cont.)

- The choice of the working point
- Linear Imperfections and correction
  - Steering error, closed orbit distortion
  - Gradient error
  - Linear coupling
- Chromaticity
- Non-linear effects
  - Kinematic effect
  - Fringe-fields
  - Magnet imperfections

Outline (cont.)

- Non-linear correction
  - Sextupole correction
  - Octupole correction
  - Error compensation in magnet design
  - Dynamic aperture
- Scaling law for magnet fringe-fields
- Frequency maps

Why care about single particle dynamics?

- Accelerator design focuses on high performance
- In the case of high-intensity rings, the goal is a “low-loss” design
- Losses in the high-intensity are due to the combination of space-charge and magnetic field errors
- Large transverse emittance in high-intensity low-energy rings amplifies error effects

$$\downarrow$$

Identification of magnet errors and non-linearities and correction

The single-particle relativistic Hamiltonian

$$H(\mathbf{x}, \mathbf{p}, t) = c\sqrt{\left(\mathbf{p} - \frac{e}{c}\mathbf{A}(\mathbf{x}, t)\right)^2 + m^2c^2} + e\Phi(\mathbf{x}, t)$$

- $\mathbf{x} = (x, y, z)$ Cartesian positions
- $\mathbf{p} = (p_x, p_y, p_z)$ conjugate momenta
- $\mathbf{A} = (A_x, A_y, A_z)$ the magnetic vector potential
- Φ the electric scalar potential
- c and e velocity of light and particle charge

The ordinary kinetic momentum vector

$$\mathbf{P} = \gamma m \mathbf{v} = \mathbf{p} - \frac{e}{c}\mathbf{A}$$

with $\mathbf{v}$ the particle velocity and $\gamma = (1 - v^2/c^2)^{-1/2}$ the relativistic factor.

The single-particle relativistic Hamiltonian (cont.)

The Hamiltonian is the total energy

$$H \equiv E = \gamma m c^2 + e\Phi$$

The total kinetic momentum

$$P = \left(\frac{H^2}{c^2} - m^2 c^2 \right)^{1/2}$$

Use Hamilton's equations $(\dot{\mathbf{x}}, \dot{\mathbf{p}}) = [(\mathbf{x}, \mathbf{p}), H]$ to get equations of motion

$$\Downarrow$$

$$\boxed{\text{Lorenz equations}}$$

The single-particle relativistic Hamiltonian (cont.)

Canonical Transformation **I**: $(x, y, z, p_x, p_y, p_z) \mapsto (x, y, s, p_x, p_y, p_s)$

moving the coordinate system on a closed curve, with path length s, of a particle with reference momentum P_0 in the guiding magnetic field.

The new Hamiltonian

$$H(\mathbf{x}', \mathbf{p}', t) = c\sqrt{(p_x - \frac{e}{c}A_x)^2 + (p_y - \frac{e}{c}A_x)^2 + \frac{(p_s - \frac{e}{c}A_s)^2}{(1 + \frac{x}{\rho(s)})^2} + m^2c^2} + e\Phi(\mathbf{x}')$$

- $A_s = (\mathbf{A} \cdot \hat{\mathbf{s}})(1 + \frac{x}{\rho(s)})$
- $p_s = (\mathbf{p} \cdot \hat{\mathbf{s}})(1 + \frac{x}{\rho(s)})$
- $\rho(s)$ the local radius of curvature

The single-particle relativistic Hamiltonian (cont.)

Canonical Transformation **II**: $(x, y, s, p_x, p_y, p_s) \mapsto (x, y, t, p_x, p_y, -H)$

setting the path s as the independent variable and the momentum $-p_s$ as the new Hamiltonian. Assuming $\Phi = 0$

$$\mathcal{H} \equiv (-p_s) = -\frac{e}{c}A_s - \left(1 + \frac{x}{\rho(s)}\right)\sqrt{\frac{H^2}{c^2} - m^2c^2 - (p_x - \frac{e}{c}A_x)^2 - (p_y - \frac{e}{c}A_y)^2}$$

If $\mathbf{A}$ time independent $\longrightarrow \mathcal{H}$ integral of motion, i.e. constant along the particle trajectories.

$\star\star\star$ Longitudinal motion neglected (not valid for RSC's) $\star\star\star$

Linear betatron motion

Assume a simple case of linear transverse fields:

$$\begin{aligned} B_x &= \quad b_1(s)y \\ B_y &= -b_0(s) + b_1(s)x \end{aligned} \quad ,$$

- main bending field $B_0 \equiv b_0(s) = \frac{P_0 c}{e\rho(s)}$ [T]
- normalized quadrupole gradient $K(s) = b_1(s)\frac{e}{cP_0} = \frac{b_1(s)}{B\rho}$ [$1/\mathrm{m}^2$]
- magnetic rigidity $B\rho = \dfrac{P_0 c}{e}$ [$\mathrm{T} \cdot \mathrm{m}$]

The vector potential $\mathbf{A} = (0, 0, A_s)$ with

$$A_s(x, y, s) = -\frac{P_0 c}{e}\left[\frac{x}{\rho(s)} + \left(\frac{1}{\rho(s)^2} - K(s)\right)\frac{x^2}{2} + K(s)\frac{y^2}{2}\right] \quad .$$

Linear betatron motion (cont.)

The Hamiltonian can be written as:

$$\mathcal{H} = -P_0\left[\frac{x}{\rho(s)} + \left(\frac{1}{\rho^2} - K(s)\right)\frac{x^2}{2} + K(s)\frac{y^2}{2}\right] - \left(1 + \frac{x}{\rho(s)}\right)\sqrt{P^2 - p_x^2 - p_y^2}$$

Equations of motion still non-linear in the canonical momenta!

- Canonical transformation **III**: $(p_x, p_y, -H) \mapsto (\frac{p_x}{P}, \frac{p_y}{P}, \frac{-H}{P})$ rescaling the canonical momenta
- Expand the square root
- Throw away terms higher than quadratic (not always a good idea!)
- Introduce the momentum spread $\delta = \frac{\delta P}{P_0} = (\frac{P-P_0}{P_0})$
- new canonical momentum $p_x = \frac{dx}{ds} \equiv x'$

Linear betatron motion (cont.)

The new Hamiltonian:

$$\hat{\mathcal{H}} \equiv (-p_s/P) = \frac{1}{2}\left(p_x^2 + p_y^2\right) + \frac{\delta}{1+\delta}\frac{x}{\rho(s)} + \frac{1}{1+\delta}\left[\left(\frac{1}{\rho(s)^2} - K(s)\right)\frac{x^2}{2} + K(s)\frac{y^2}{2}\right]$$

Hill's equations of betatron motion

$$x'' + \frac{1}{1+\delta}\left(\frac{1}{\rho(s)^2} - K(s)\right)x = \frac{\delta}{1+\delta}\frac{1}{\rho(s)}$$

$$y'' + \frac{1}{1+\delta}K(s)y = 0$$

Introduce dispersion function

$$D_x'' - \frac{1}{1+\delta}K_x(s)D_x = \frac{1}{\rho(s)} \quad ,$$

where $K_x(s) \equiv \dfrac{1}{\rho(s)^2} - K(s)$ and $K_y(s) \equiv K(s)$.

Linear betatron motion (cont.)

• Canonical transformation **IV**: $(x, y, p_x, p_y) \mapsto (x - x_0, y, p_x - p_{x0}, p_y)$ shifting the coordinate origin to the closed orbit.

The new equations of motion

$$x'' + K_x(s)x, = 0 \qquad , \qquad y'' + K_y(s)y = 0 \ .$$

Homogeneous equations with periodic coefficients $K_{x,y}(s) = K_{x,y}(s + C)$

Floquet Theory

$$\downarrow$$

$$x = \sqrt{A_x\beta_x(s)}\cos(\psi_x(s) + \psi_{0x}) \quad , \quad y = \sqrt{A_y\beta_y(s)}\cos(\psi_y(s) + \psi_{0y}) \ .$$

- the Courant-Snyder invariant $A_{x,y}$
- the Courant-Snyder amplitude function $\beta_{x,y}(s)$
- the alpha $\alpha_{x,y} = -\frac{\beta'_{x,y}}{2}$ and gamma $\gamma_{x,y} = \frac{1+\alpha^2_{x,y}}{\beta'_{x,y}}$ functions
- the phase advance $\psi_{x,y}(s) = \int_0^s \frac{d\tau}{\beta_{x,y}(\tau)}$
- the tunes $Q_{x,y} = \frac{1}{2\pi}\int_0^C \frac{ds}{\beta_{x,y}(s)}$

Action-angle variables

- Canonical transformation $\mathbf{V}$ to action angle variables $(\phi_x, \phi_y, J_x, J_y)$

$$x(s) = \sqrt{2\beta_x(s) J_x} \cos\left(\phi_x(s) + \theta_x(s)\right)$$

$$p_x(s) = -\sqrt{\frac{2J_x}{\beta_x(s)}} \left[\sin\left(\phi_x(s) + \theta_x(s)\right) + \alpha_x(s) \cos\left(\phi_x(s) + \theta_x(s)\right)\right]$$

with

$$\theta_x(s) = -\arctan\left[\frac{\beta_x(s)x' + \alpha_x(s)x}{x}\right] - \phi_x(s) \quad .$$

The new Hamiltonian

$$H_0(J_x, J_y) = \frac{1}{R}(Q_x J_x + Q_y J_y) \quad ,$$

The equations of motion

$$J_x = \text{constant} \quad , \qquad J_y = \text{constant}$$

$$\phi_x(s) = \phi_{x0}(s) + \frac{Q_x(s - s_0)}{R} \quad , \qquad \phi_y(s) = \phi_{y0}(s) + \frac{Q_y(s - s_0)}{R} \quad ,$$

and describe a 2-torus in the phase space $(\phi_x, \phi_y, J_x, J_y)$.

Generalized "non-integrable" Hamiltonian

- Transverse vector potential:
  - Basic law of magnetostatics $\boldsymbol{\nabla} \cdot \boldsymbol{B} = 0 \longrightarrow \exists\, \boldsymbol{A} \;: \boldsymbol{B} = \boldsymbol{\nabla} \times \boldsymbol{A}$
  - Ampére's law in vacuum $\boldsymbol{\nabla} \times \boldsymbol{B} = 0 \longrightarrow \exists\, V \;: \boldsymbol{B} = \boldsymbol{\nabla} V$

$$B_x = -\frac{\partial V}{\partial x} = \frac{\partial A_z}{\partial y} \qquad , \qquad B_y = -\frac{\partial V}{\partial y} = \frac{\partial A_z}{\partial s}$$

$$\uparrow$$

Cauchy-Riemann conditions of analytic functions

$$\downarrow$$

$$\mathcal{A}(x+iy) = A_z(x,y) + iV(x,y) = \sum_{n=1}^{\infty} (\kappa_n + i\lambda_n)(x+iy)^n$$

The normal and skew multipole coefficients

$$b_{n-1} = -\frac{n\kappa_n r_0^{n-1}}{B_0} \qquad \text{and} \qquad a_{n-1} = \frac{n\lambda_n r_0^{n-1}}{B_0}$$

with r_0 the reference radius, B_0 the main field

Generalized “non-integrable” Hamiltonian (cont.)

- The Hamiltonian:

$$\mathcal{H} \equiv (-p_s/P) = \frac{1}{2}\left(p_x^2 + p_y^2\right) - \frac{x}{\rho(s)} - \frac{e}{cP}A_s$$

The vector potential component A_s is:

$$A_s = (\mathbf{A}\cdot\hat{\mathbf{s}})(1+\frac{x}{\rho(s)})$$

$$= (1+\frac{x}{\rho(s)})B_0\Re e\sum_{n=0}^{\infty}\frac{b'_n + ia'_n}{n}(x+iy)^{n+1}$$

Use transformation **IV** $x = x_\beta + D_x\delta + x_0,\ y = y_\beta + D_y\delta + y_0$

The new Hamiltonian is

$$\mathcal{H}' = H_0 + \sum_{k_x,k_y} h_{k_x,k_y}(s)x^{k_x}y^{k_y}$$

where H_0 is the integrable Hamiltonian. The terms $h_{k_x,k_y}(s)$ are periodic and depend on a'_n, b'_n and the closed orbit displacements $\Delta_x = D_x\delta + x_0,\ \Delta_y = D_y\delta + y_0$

Classical perturbation theory

(Linstead (1882), Poincaré (1892), Von-Zeipel (1916))

Consider a general Hamiltonian with n degrees of freedom

$$H(\boldsymbol{J},\boldsymbol{\varphi},\theta) = H_0(\mathbf{J}) + \epsilon H_1(\boldsymbol{J},\boldsymbol{\varphi},\theta) + \mathcal{O}(\epsilon^2)$$

where the non-integrable part $H_1(\boldsymbol{J},\boldsymbol{\varphi},\theta)$ is 2π-periodic on θ and φ.

If ϵ small $\longrightarrow$ distorted tori still exist $\longrightarrow$ try to "streighten up" the tori

$$\downarrow$$

Canonical Transformation **VI**: Search a generating function

$$S(\bar{\boldsymbol{J}},\boldsymbol{\varphi},\theta) = \bar{\boldsymbol{J}}\cdot\boldsymbol{\varphi} + \epsilon S_1(\bar{\boldsymbol{J}},\boldsymbol{\varphi},\theta) + \mathcal{O}(\epsilon^2)$$

for transforming old variables to $(\bar{\boldsymbol{J}},\bar{\boldsymbol{\varphi}})$ so that new $\bar{H}(\bar{\boldsymbol{J}})$ only a function of the new actions.

Classical perturbation theory (cont.)

By the canonical transformation equations, the old action and new angle are:

$$\boldsymbol{J} = \bar{\boldsymbol{J}} + \epsilon \frac{\partial S_1(\bar{\boldsymbol{J}}, \boldsymbol{\varphi}, \theta)}{\partial \boldsymbol{\varphi}} + \mathcal{O}(\epsilon^2)$$

$$\bar{\boldsymbol{\varphi}} = \boldsymbol{\varphi} + \epsilon \frac{\partial S_1(\bar{\boldsymbol{J}}, \boldsymbol{\varphi}, \theta)}{\partial \bar{\boldsymbol{J}}} + \mathcal{O}(\epsilon^2)$$

Inverting the previous equations:

$$\boldsymbol{J} = \bar{\boldsymbol{J}} + \epsilon \frac{\partial S_1(\bar{\boldsymbol{J}}, \bar{\boldsymbol{\varphi}}, \theta)}{\partial \bar{\boldsymbol{\varphi}}} + \mathcal{O}(\epsilon^2)$$

$$\boldsymbol{\varphi} = \bar{\boldsymbol{\varphi}} - \epsilon \frac{\partial S_1(\bar{\boldsymbol{J}}, \bar{\boldsymbol{\varphi}}, \theta)}{\partial \bar{\boldsymbol{J}}} + \mathcal{O}(\epsilon^2)$$

$\star\star\star$ S_1 is expressed in terms of the new variables $\star\star\star$

Classical perturbation theory (cont.)

The new Hamiltonian is:

$$\bar{H}(\bar{\boldsymbol{J}}, \bar{\boldsymbol{\varphi}}, \theta) = H(\boldsymbol{J}(\bar{\boldsymbol{J}}, \bar{\boldsymbol{\varphi}}), \boldsymbol{\varphi}(\bar{\boldsymbol{J}}, \bar{\boldsymbol{\varphi}}), \theta) + \epsilon \frac{\partial S_1(\bar{\boldsymbol{J}}, \bar{\boldsymbol{\varphi}}, \theta)}{\partial \theta} + \mathcal{O}(\epsilon^2)$$

Expand term by term the old Hamiltonian to leading order in ϵ:

$$H_0(\boldsymbol{J}(\bar{\boldsymbol{J}}, \bar{\boldsymbol{\varphi}})) = H_0(\bar{\boldsymbol{J}}) + \epsilon \frac{\partial H_0(\bar{\boldsymbol{J}})}{\partial \bar{\boldsymbol{J}}} \frac{\partial S_1(\bar{\boldsymbol{J}}, \bar{\boldsymbol{\varphi}}, \theta)}{\partial \bar{\boldsymbol{\varphi}}} + \mathcal{O}(\epsilon^2)$$

$$\epsilon H_1(\boldsymbol{J}(\bar{\boldsymbol{J}}, \bar{\boldsymbol{\varphi}}), \boldsymbol{\varphi}(\bar{\boldsymbol{J}}, \bar{\boldsymbol{\varphi}}), \theta) = \epsilon H_1(\bar{\boldsymbol{J}}, \bar{\boldsymbol{\varphi}}) + \mathcal{O}(\epsilon^2)$$

Equating the terms of equal order in ϵ, we get in zero order $\bar{H}_0 = H_0(\bar{\boldsymbol{J}})$ and in first order:

$$\bar{H}_1 = \frac{\partial S_1(\bar{\boldsymbol{J}}, \bar{\boldsymbol{\varphi}}, \theta)}{\partial \theta} + \boldsymbol{\omega}(\bar{\boldsymbol{J}}) \cdot \frac{\partial S_1(\bar{\boldsymbol{J}}, \bar{\boldsymbol{\varphi}}, \theta)}{\partial \bar{\boldsymbol{\varphi}}} + H_1(\bar{\boldsymbol{J}}, \bar{\boldsymbol{\varphi}})$$

with $\boldsymbol{\omega}(\bar{\boldsymbol{J}}) = \dfrac{\partial H_0(\bar{\boldsymbol{J}})}{\partial \bar{\boldsymbol{J}}}$ the unperturbed frequency vector.

Classical perturbation theory (cont.)

New Hamiltonian should be a function of $\bar{\boldsymbol{J}}$ only $\longrightarrow$ eliminate $\bar{\boldsymbol{\varphi}}$

$$\downarrow$$

- Average part: $\langle H_1 \rangle_{\bar{\boldsymbol{\varphi}}} = \left(\frac{1}{2\pi}\right)^n \oint H_1(\bar{\boldsymbol{J}}, \bar{\boldsymbol{\varphi}}) d\bar{\boldsymbol{\varphi}}$
- Oscillating part: $\{H_1\} = H_1 - \langle H_1 \rangle_{\bar{\boldsymbol{\varphi}}}$

Using the previous equations, $\bar{H}_1$ becomes

$$\bar{H}_1 = \frac{\partial S_1(\bar{\boldsymbol{J}}, \bar{\boldsymbol{\varphi}}, \theta)}{\partial \theta} + \boldsymbol{\omega}(\bar{\boldsymbol{J}}) \cdot \frac{\partial S_1(\bar{\boldsymbol{J}}, \bar{\boldsymbol{\varphi}}, \theta)}{\partial \bar{\boldsymbol{\varphi}}} + \langle H_1(\bar{\boldsymbol{J}}, \bar{\boldsymbol{\varphi}}) \rangle_{\bar{\boldsymbol{\varphi}}} + \{H_1(\bar{\boldsymbol{J}}, \bar{\boldsymbol{\varphi}})\} \ .$$

Classical perturbation theory (cont.)

Choose S_1 so that $\bar{\varphi}$ dependence is eliminated:

$$\bar{H}_1(\bar{\boldsymbol{J}}) = \langle H_1(\bar{\boldsymbol{J}}, \bar{\boldsymbol{\varphi}})\rangle_{\bar{\boldsymbol{\varphi}}} \quad \text{and} \quad \frac{\partial S_1(\bar{\boldsymbol{J}}, \bar{\boldsymbol{\varphi}}, \theta)}{\partial \theta} + \boldsymbol{\omega}(\bar{\boldsymbol{J}}) \cdot \frac{\partial S_1(\bar{\boldsymbol{J}}, \bar{\boldsymbol{\varphi}}, \theta)}{\partial \bar{\boldsymbol{\varphi}}} = -\{H_1(\bar{\boldsymbol{J}}, \bar{\boldsymbol{\varphi}})\} \ ,$$

New Hamiltonian is a function of the new actions only to leading order!!!

$$\bar{H}(\bar{\boldsymbol{J}}) = H_0(\bar{\boldsymbol{J}}) + \epsilon \, \langle H_1(\bar{\boldsymbol{J}}, \bar{\boldsymbol{\varphi}})\rangle_{\bar{\boldsymbol{\varphi}}} + \mathcal{O}(\epsilon^2) \ ,$$

with the new frequency vector

$$\bar{\boldsymbol{\omega}}(\bar{\boldsymbol{J}}) = \frac{\partial \bar{H}(\bar{\boldsymbol{J}})}{\partial \bar{\boldsymbol{J}}} = \boldsymbol{\omega}(\bar{\boldsymbol{J}}) + \epsilon \frac{\partial \langle H_1(\bar{\boldsymbol{J}}, \bar{\boldsymbol{\varphi}})\rangle_{\bar{\boldsymbol{\varphi}}}}{\partial \bar{\boldsymbol{J}}} + \mathcal{O}(\epsilon^2) \ .$$

Classical perturbation theory (cont.)

BUT can we find an appropriate generating function S_1?

$$\downarrow$$

Expand in Fourier series

$$\{H_1(\bar{\boldsymbol{J}}, \bar{\boldsymbol{\varphi}})\} = \sum_{\boldsymbol{k},p} H_{1\mathbf{k}}(\bar{\boldsymbol{J}}) e^{i(\boldsymbol{k}\cdot\bar{\boldsymbol{\varphi}}+p\theta)} \quad ,$$

with $\boldsymbol{k}\cdot\bar{\boldsymbol{\varphi}} = k_1\bar{\varphi_1} + \cdots + k_n\bar{\varphi_n}$. and also

$$S_1(\bar{\boldsymbol{J}}, \bar{\boldsymbol{\varphi}}, \theta) = \sum_{\boldsymbol{k},p} S_{1\mathbf{k}}(\bar{\boldsymbol{J}}) e^{i(\boldsymbol{k}\cdot\bar{\boldsymbol{\varphi}}+p\theta)} \quad .$$

The unknown amplitudes $S_{1k}(\bar{\boldsymbol{J}})$ are:

$$S_{1k}(\bar{\boldsymbol{J}}) = i\frac{H_{1k}(\bar{\boldsymbol{J}})}{\boldsymbol{k}\cdot\boldsymbol{\omega}(\bar{\boldsymbol{J}})+p} \qquad \text{with} \qquad \boldsymbol{k}, p \neq \mathbf{0} \quad ,$$

and finally

$$S(\bar{\boldsymbol{J}}, \bar{\boldsymbol{\varphi}}) = \bar{\boldsymbol{J}}\cdot\bar{\boldsymbol{\varphi}} + \epsilon i \sum_{\mathbf{k}\neq\mathbf{0}} \frac{H_{1\mathbf{k}}(\bar{\mathbf{J}})}{\boldsymbol{k}\cdot\boldsymbol{\omega}(\bar{\boldsymbol{J}})+p} e^{i(\boldsymbol{k}\cdot\bar{\boldsymbol{\varphi}}+p\theta)} + \mathcal{O}(\epsilon^2) \quad .$$

Classical perturbation theory (cont.)

- Remarks

1) What about higher orders?

In principle, the technique works for arbitrary order, **but** variables disentagling becomes difficult (even for 2nd order!!!)

$$\downarrow$$

Solution $\longrightarrow$ Lie transformations

(Application in beam dynamics by Dragt and Finn (1976))

2) What about small denominators?

Resonances $\boldsymbol{k} \cdot \boldsymbol{\omega}(\bar{\boldsymbol{J}}) + p = 0$

$$\downarrow$$

Solution $\longrightarrow$ Superconvergent perturbation techniques - KAM theory

(Kolmogorov (1957), Arnold (1962) and Moser (1962))

Application to the accelerator Hamiltonian

(Hagedorn (1957), Schoch (1957), Guignard (1976, 1978))

- The general acceleretor Hamiltonian:

$$\mathcal{H}'(J_x, J_y, \phi_x, \phi_y) = H_0(J_x, J_y) + H_1(J_x, J_y, \phi_x, \phi_y)$$

The transverse variable:

$$x(s) = \sqrt{\frac{J_x \beta_x(s)}{2}} \left(e^{i(\phi_x(s)+\theta_x(s))} + e^{-i(\phi_x(s)+\theta_x(s))} \right)$$

and the equivalent y. The Hamiltonian in action-angle variables:

$$\mathcal{H}'(J_x, J_y, \phi_x, \phi_y) = H_0(J_x, J_y) + H_1(J_x, J_y, \phi_x, \phi_y)$$

- The integrable part $H_0(J_x, J_y) = \frac{1}{R}(Q_x J_x + Q_y J_y)$
- The perturbation

$$H_1(J_x, J_y, \phi_x, \phi_y; s) = \sum_{k_x, k_y} J_x^{k_x/2} J_y^{k_y/2} \sum_j^{k_x} \sum_l^{k_y} g_{j,k,l,m}(s) e^{i[(j-k)\phi_x + (l-m)\phi_y]}$$

- The coefficients

$$g_{j,k,l,m}(s) = \frac{h_{k_x,k_y}(s)}{2^{\frac{j+k+l+m}{2}}} \binom{k_x}{j} \binom{k_y}{l} \beta_x^{k_x/2}(s) \beta_y^{k_y/2}(s) e^{i[(j-k)\theta_x(s) + (l-m)\theta_y(s)]}$$

- The indexes j, k, l, m: $k_x = j + k$ and $k_y = l + m$.

Resonance driving terms

Coefficients $h_{k_x,k_y}(s)$ are periodic in $\theta \longrightarrow$ expand in Fourier series

$$H_1(J_x, J_y, \phi_x, \phi_y; s) = \sum_{k_x,k_y} J_x^{k_x/2} J_y^{k_y/2} \sum_j^{k_x} \sum_l^{k_y} \sum_{p=-\infty}^{\infty} g_{j,k,l,m;p} e^{i[(j-k)\phi_x + (l-m)\phi_y - p\frac{s}{R}]}$$

with the **resonance driving terms**

$$g_{j,k,l,m;p} = \binom{k_x}{j}\binom{k_y}{l} \frac{1}{2^{\frac{j+k+l+m}{2}}} \frac{1}{2\pi} \oint h_{k_x,k_y}(s) \beta_x^{k_x/2}(s) \beta_y^{k_y/2}(s) e^{i[(j-k)\theta_x(s) + (l-m)\theta_y(s) + p\frac{s}{R}]}$$

For $n_x = j - k$ and $n_y = l - m$ we have the resonance conditions

$n_x Q_x + n_y Q_y = p$.

Goal of accelerator design and correction systems $\longrightarrow$ minimize $g_{j,k,l,m;p}$ by

- Change magnet design so that $h_{k_x,k_y}(s)$ become smaller
- Introduce magnetic elements capable of creating a cancelling effect

Tune-shift and spread

First order correction to the tunes $\longrightarrow$ derivatives with respect to the action of average part of H_1. For a given term $h_{k_x,k_y}(s)x^{k_x}y^{k_y}$:

$$\delta Q_x = \frac{J_x^{k_x/2-1} J_y^{k_y/2}}{4\pi^2} \sum_j^{k_x} \sum_l^{k_y} \bar{g}_{j,k,l,m} \oint e^{i[(j-k)\phi_x+(l-m)\phi_y]}$$

$$\delta Q_y = \frac{J_x^{k_x/2} J_y^{k_y/2-1}}{4\pi^2} \sum_j^{k_x} \sum_l^{k_y} \bar{g}_{j,k,l,m} \oint e^{i[(j-k)\phi_x+(l-m)\phi_y]}$$

where $\bar{g}_{j,k,l,m}$ the average of $g_{j,k,l,m}(s)$ around the ring.

- Remarks
  - If $\delta Q_{x,y}$ independent of $J_{x,y}$ $\longrightarrow$ tune-shift
  - If $\delta Q_{x,y}$ depends on $J_{x,y}$ $\longrightarrow$ tune-spread (or amplitude detuning)
  - $\delta Q_{x,y} = 0$ for $k_x = j + k$ or $k_y = l + m$ odd $\longrightarrow$ go to higher order
  - Leading order tune-shift $\longrightarrow$ impact of errors and non-linear effects

Tune-shift and spread (cont.)

Table 1: Tune spread produced by various mechanisms on a 2 MW beam with transverse emittance of 480 π mm mrad and momentum spread of $\pm 1\%$.

Mechanism	Full tune spread
Space charge	0.15-0.2 (2 MW beam)
Chromaticity	$\pm$0.08 (1% $\Delta\ p/p$)
Kinematic nonlinearity (480π)	0.001
Fringe field (480π)	0.025
Uncompensated ring magnet error (480π)	$\pm$0.02
Compensated ring magnet error (480π)	$\pm$0.002
Fixed injection chicane	0.004
Injection painting bump	0.001

The single resonance treatment

General two dimensional Hamiltonian:

$$H(\mathbf{J}, \boldsymbol{\varphi}) = H_0(\mathbf{J}) + \varepsilon H_1(\mathbf{J}, \boldsymbol{\varphi})$$

with the perturbed part periodic in angles:

$$H_1(\mathbf{J}, \boldsymbol{\varphi}) = \sum_{k_1,k_1} H_{k_1,k_2}(J_1, J_2) \exp[i(k_1\varphi_1 + k_2\varphi_2)]$$

Resonance $n_1\omega_1 + n_2\omega_2 = 0 \longrightarrow$ blow up the solution

$$\downarrow$$

Canonical transformation **VII**: $(\mathbf{J}, \boldsymbol{\varphi}) \longmapsto (\hat{\mathbf{J}}, \hat{\varphi})$ eliminate one action:

$$F_r(\hat{\mathbf{J}}, \boldsymbol{\varphi}) = (n_1\varphi_1 - n_2\varphi_2)\hat{J}_1 + \varphi_2\hat{J}_2$$

The transformed Hamiltonian

$$\hat{H}(\hat{\mathbf{J}}, \hat{\boldsymbol{\varphi}}) = \hat{H}_0(\hat{\mathbf{J}}) + \varepsilon\hat{H}_1(\hat{\mathbf{J}}, \hat{\boldsymbol{\varphi}})$$

ant the perturbation

$$\hat{H}_1(\hat{\mathbf{J}}, \hat{\boldsymbol{\varphi}}) = \sum_{k_1,k_2} H_{k_1,k_2}(\hat{\mathbf{J}}) \exp\left\{\frac{i}{n_1}\left[k_1\hat{\varphi}_1 + (k_1 n_2 + k_2 n_1)\hat{\varphi}_1\right]\right\}$$

The single resonance treatment (cont.)

Relations between the variables

$$\begin{aligned} J_1 &= n_1 \hat{J}_1 \quad , \qquad J_2 = \hat{J}_2 - n_2 \hat{J}_1 \\ \hat{\varphi}_1 &= n_1\varphi_1 - n_2\varphi_2 \quad , \qquad \hat{\varphi}_2 = \varphi_2 \end{aligned} .$$

Transformation to a rotating frame where $\dot{\hat{\varphi}}_1 = n_1\dot{\varphi}_1 - n_2\dot{\varphi}_2$ measures deviation from resonance.

Average over the "slow" angle $\hat{\varphi}_2 = \varphi_2$

$$\bar{H}(\hat{\mathbf{J}}, \hat{\boldsymbol{\varphi}}) = \bar{H}_0(\hat{\mathbf{J}}) + \varepsilon \bar{H}_1(\hat{\mathbf{J}}, \hat{\varphi}_1)$$

with $\bar{H}_0(\hat{\mathbf{J}}) = \hat{H}_0(\hat{\mathbf{J}})$ and

$\bar{H}_1(\hat{\mathbf{J}}, \hat{\varphi}_1) = \langle \hat{H}_1(\hat{\mathbf{J}}, \hat{\varphi}_1) \rangle_{\hat{\varphi}_2} = \sum_{p=-\infty}^{+\infty} H_{-pn_1, pn_2}(\hat{\mathbf{J}}) \exp(-ip\hat{\varphi}_1)$

The averaging eliminated one angle and thus $\hat{J}_2 = J_2 + J_1\frac{n_2}{n_1}$ is an invariant of motion.

The single resonance treatment (cont.)

Assume dominant Fourier harmonics for $p = 0, \pm 1$

$$\bar{H}(\hat{\mathbf{J}}, \hat{\theta}_1) = \bar{H}_0(\hat{\mathbf{J}}) + \varepsilon \bar{H}_{0,0}(\hat{\mathbf{J}}) + 2\varepsilon \bar{H}_{n_1,-n_2}(\hat{\mathbf{J}}) \cos \hat{\varphi}_1$$

Introduce $\Delta \hat{J}_1 = \hat{J}_1 - \hat{J}_{10}$ moving reference on fixed point and expand $\bar{H}(\hat{\mathbf{J}})$ around it $\rightarrow$ Hamiltonian describing motion near a resonance:

$$\bar{H}_r(\Delta \hat{J}_1, \hat{\theta}_1) = \left.\frac{\partial^2 \bar{H}_0(\hat{\mathbf{J}})}{\partial \hat{J}_1^{\,2}}\right|_{\hat{J}_1 = \hat{J}_{10}} \frac{(\Delta \hat{J}_1)^2}{2} + 2\varepsilon \bar{H}_{n_1,-n_2}(\hat{\mathbf{J}}) \cos \hat{\varphi}_1$$

Motion near a typical resonance is like that of the pendulum!!!

The libration frequency

$$\hat{\omega}_1 = \left(2\varepsilon \bar{H}_{n_1,-n_2}(\hat{\mathbf{J}}) \left.\frac{\partial^2 \bar{H}_0(\hat{\mathbf{J}})}{\partial \hat{J}_1^{\,2}}\right|_{\hat{J}_1 = \hat{J}_{10}} \right)^{1/2}$$

The resonance half width

$$\Delta \hat{J}_{1\ max} = 2 \left(\frac{2\varepsilon \bar{H}_{n_1,-n_2}(\hat{\mathbf{J}})}{\left.\frac{\partial^2 \bar{H}_0(\hat{\mathbf{J}})}{\partial \hat{J}_1^{\,2}}\right|_{\hat{J}_1 = \hat{J}_{10}}} \right)^{1/2}$$

Resonance overlap criterion

(Chirikov (1960, 1979) Contopoulos (1966))

When perturbation grows $\longrightarrow$ width of resonance island grows.

$$\downarrow$$

Rwo resonant islands overlap $\longrightarrow$ orbits diffuse through the resonances.

Distance between two resonances

$$\delta \hat{J}_{1\ n,n'} = \frac{2\left(\frac{1}{n_1+n_2} - \frac{1}{n'_1+n'_2}\right)}{\left|\frac{\partial^2 \bar{H}_0(\hat{\mathbf{J}})}{\partial \hat{J}_1^{\,2}}\Big|_{\hat{J}_1=\hat{J}_{10}}\right|}$$

we get a simple resonance overlap criterion $\Delta \hat{J}_{n\ max} + \Delta \hat{J}_{n'\ max} \geq \delta \hat{J}_{n,n'}$

Considering width of chaotic layer and secondary islands, we have the "two thirds" rule $\Delta \hat{J}_{n\ max} + \Delta \hat{J}_{n'\ max} \geq \frac{2}{3}\delta \hat{J}_{n,n'}$

Limitation: geometrical nature $\longrightarrow$ difficult to extend in systems with $n \geq 3$

Single resonance theory for the accelerator Hamiltonian

(Hagedorn (1957), Schoch (1957), Guignard (1976, 1978))

The single resonance accelerator Hamiltonian

$$
\begin{aligned}
H(J_x, J_y, \phi_x, \phi_y, s) = & \frac{1}{R}(Q_x J_x + Q_y J_y) \\
& + g_{n_x,n_y} \frac{2}{R} J_x^{\frac{k_x}{2}} J_y^{\frac{k_y}{2}} \cos(n_x\phi_x + n_y\phi_y + \phi_0 - p\frac{s}{R})
\end{aligned}
$$

with $g_{n_x,n_y} e^{i\phi_0} = g_{j,k,l,m;p}$.

From the generating function

$$
F_r(\phi_x, \phi_y, \hat{J}_x, \hat{J}_y, s) = (n_x\phi_x + n_y\phi_y - p\frac{s}{R})\hat{J}_x + \phi_y\hat{J}_y
$$

we get the Hamiltonian

$$
\begin{aligned}
\hat{H}(\hat{J}_x, \hat{J}_y, \phi_x) = & \frac{(n_x Q_x + n_y Q_y - p)\hat{J}_x + \hat{J}_y}{R} \\
& + g_{n_x,n_y} \frac{2}{R}(n_x\hat{J}_x)^{\frac{k_x}{2}} (n_y\hat{J}_x + \hat{J}_y)^{\frac{k_y}{2}} \cos(\hat{\phi_x} + \phi_0)
\end{aligned}
$$

Resonance widths

The two invariants are the new action and Hamiltonian. In the old variables:

$$c_1 = \frac{J_x}{n_x} - \frac{J_y}{n_y}$$

$$c_2 = (Q_x - \frac{p}{n_x+n_y})J_x + (Q_y - \frac{p}{n_x+n_y})J_y$$

$$+ 2g_{n_x,n_y} J_x^{\frac{k_x}{2}} J_y^{\frac{k_y}{2}} \cos(n_x\phi_x + n_y\phi_y + \phi_0 - p\frac{s}{R}) \ .$$

n_x,n_y with opposite sign (*difference* resonances) $\longrightarrow$ bounded motion

n_x, n_y with same sign (*sum* resonances) $\longrightarrow$ unbounded motion

$\star\star\star$ these are first order perturbation theory considerations $\star\star\star$

Distance from the resonance $e = n_xQ_x + n_yQ_y - p \longrightarrow$ *resonance stop band width* :

$$\Delta e = \frac{g_{n_x,n_y}}{R} J_x^{\frac{k_x-2}{2}} J_y^{\frac{k_y-2}{2}} (k_xn_xJ_x + k_yn_yJ_y)$$

The choice of the working point

During design, impose periodic structure stronger than 1

Resonance condition $n_x Q_x + n_y Q_y = p = mN$, with m the *super-periodicity*

If $p = mN \longrightarrow$ *structural* or *systematic* resonances

If $p \neq mN \longrightarrow$ *non-structural* or *random*

Major design points for high-intensity rings:

- Choose the working point far from structural resonances
- Prevent the break of the lattice supersymmetry

The choice of the working point (cont.)

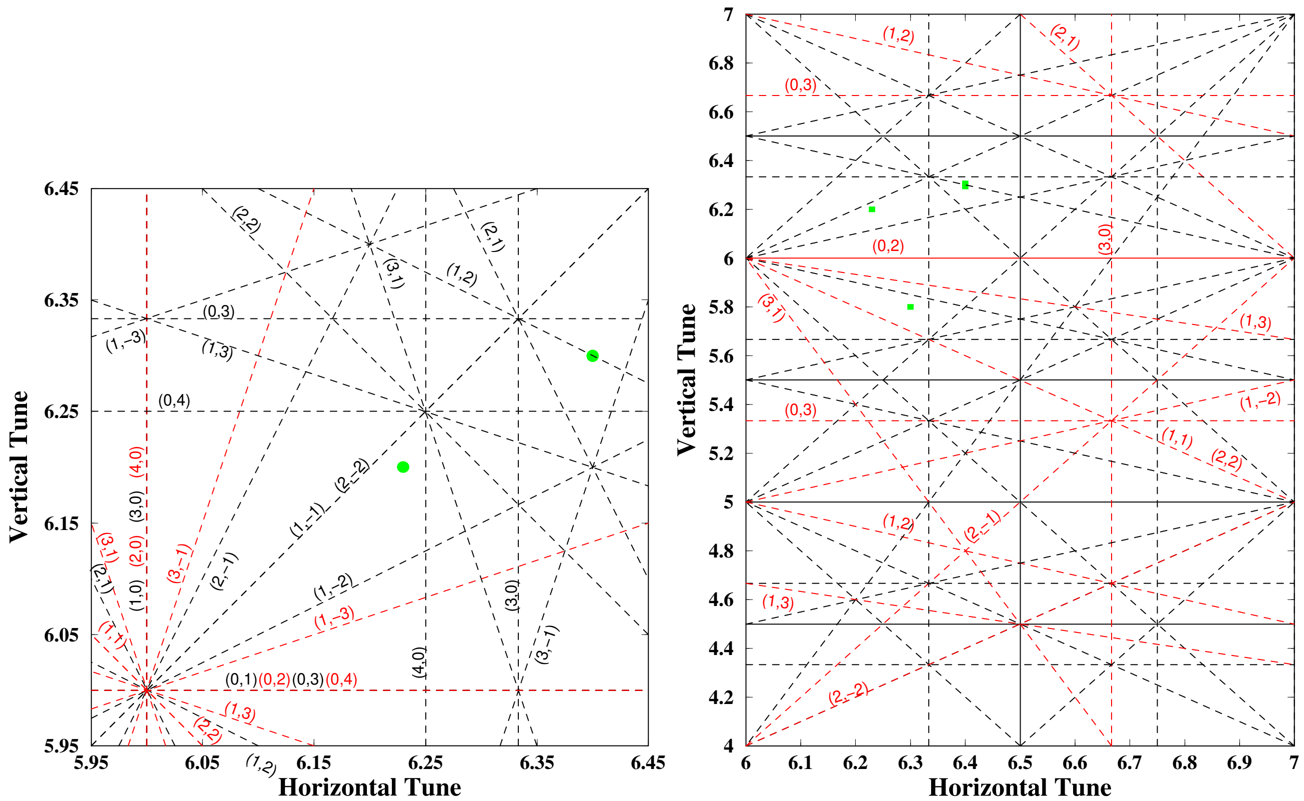

Figure 1: Tune spaces for a lattice with super-period four. The red lines are the structural resonances and the black are the non-structural (up to 4th order).

Linear Imperfections and Correction

- Steering error, closed orbit distortion
- Gradient error
- Linear coupling

- Chromaticity

Steering error and closed orbit distortion

Closed orbit control $\longrightarrow$ major concern in high intensity rings.

Effect of orbit errors: Take vector potential for a normal multi-pole and replace x and y by $x+\delta_x$ and $y+\delta_y$:

$$
\begin{aligned}
A_{n\,z}(x,y) &= -B_0 r_0 \Re e \sum_{n=0}^{\infty} \frac{b_n + i a_n}{n} \left(\frac{x+iy}{r_0}\right)^{n+1} \\
&= -\frac{B_0}{r_0^n} \frac{b_n}{n} \sum_{k=0}^{n/2} \sum_{l=0}^{n-2k} \sum_{m=0}^{2k} (-1)^l \binom{n}{2l} \binom{n-2k}{l} \binom{m}{2k} x^{n-2k-l} y^{2k-m} {\delta_x}^l {\delta_y}^m
\end{aligned}
$$

$\downarrow$

multi-pole "feed-down"

Steering error and closed orbit distortion (cont.)

Horizontal-vertical orbit distortion (Courant and Snyder 1957)

$$\delta_{x,y}(s) = -\frac{\sqrt{\beta_{x,y}}}{2\sin(\pi Q_{x,y})}\int_s^{s+C}\frac{\Delta B(\tau)}{B\rho}\sqrt{\beta_{x,y}}\cos(|\pi Q_{x,y}+\psi_{x,y}(s)-\psi_{x,y}(\tau)|)d\tau$$

with $\Delta B(\tau)$ the equivalent magnetic field error at $s = \tau$.

Approximate errors as delta functions in n locations:

$$\delta_{x,y;i} = -\frac{\sqrt{\beta_{x,y;i}}}{2\sin(\pi Q_{x,y})}\sum_{j=i+1}^{i+n}\phi_{x,y;j}\sqrt{\beta_{x,y;j}}\cos(|\pi Q_{x,y}+\psi_{x,y;i}-\psi_{x,y;j}|)$$

with $\phi_{x,y;j}$ kick produced by jth element:

- $\phi_j = \frac{\Delta B_j L_j}{B\rho} \rightarrow$ dipole field error
- $\phi_j = \frac{B_j L_j \sin\theta_j}{B\rho} \rightarrow$ dipole roll
- $\phi_j = \frac{G_j L_j \Delta x, y_j}{B\rho} \rightarrow$ quadrupole displacement

Closed orbit correction

- Introduce dipole correctors horizontal/vertical located in horizontal/vertical high beta's
- Introduce random distributions of errors (for simulations)
- Monitor $\delta_{x,y;i}$ in BPM's (virtual, for simulations)
- Minimize $\delta_{x,y;i}$ globally
- Use *three-bumps* method $\longrightarrow$ for local correction (or alternative four-bumps)

Closed orbit correction (cont.)

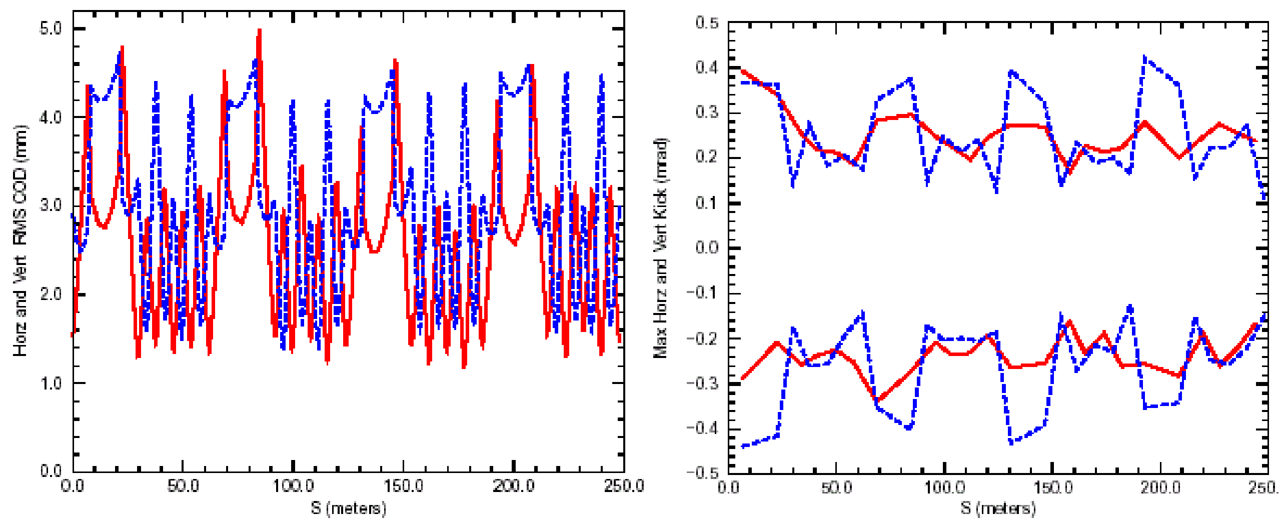

Figure 2: Horizontal and vertical closed orbit rms displacement for 101 error distributions in the SNS accumulator ring and maximum kicks required for correction (courtesy of C.J. Gardner)

Gradient error

Key issue for good performance $\longrightarrow$ super-periodicity preservation

$\downarrow$

Only structural resonances are excited

Broken super-periodicity (e.g. by random errors) $\longrightarrow$ non-structural resonances

$\downarrow$

Excessive beam loss

Causes:

- Errors in quadrupole strengths (random ans systematic)
- Injection devices
- Higher order multi-pole magnets and errors

Gradient error (cont.)

- Observables
  - Distortion of the tune

$$\delta Q_{x,y} = \frac{1}{4\pi} \oint \beta_{x,y}(s) \delta K_{x,y}(s) ds$$

  - Distortion of the optics functions, e.g. beta variation

$$\frac{\delta\beta_{x,y}(s)}{\beta_{x,y}(s)} = -\frac{1}{2\sin(2\pi Q_{x,y})} \int_s^{s+C} \beta_{x,y}(\tau)\delta K_{x,y}(\tau)\cos[-2(\pi Q_{x,y} + \psi x, y(s) - \psi x, y(\tau))]d\tau$$

  - Integer $Q_{x,y} = N$ and half-integer resonances $2Q_{x,y} = N$

Gradient error correction

- Introduce TRIM windings on the core of quadrupoles
- Introduce random distributions of quadrupole errors (for simulations)
- Monitor $\delta Q_{x,y}$ tune-shift in tune-meter (virtual, for simulations)
- Monitor $\frac{\delta\beta_{x,y}(s)}{\beta_{x,y}(s)}$ with BPM's turn-by-turn data (virtual)
- Retune the lattice and minimize beta distortions (especially in areas of maximum beta and dispersion) with TRIM windings
- Move working point close to integer, half-integer resonances
- Minimize beta wave (or resonance stop-band width)

Remarks:

- To excite/correct certain resonance harmonic N, strings powered accordingly
- Individual powering of TRIM windings for flexibility and beam based alignement of BPMs

Linear coupling and correction

Betatron motion eqs. $\longrightarrow$ coupled linear oscillators (xy term in A_s)

Effect:

- Tune-shift
- Optics function distortion
- Coupling resonances excitation $Q_x \pm Q_y = N$ and beam loss

Causes:

- Random rolls in the quadrupoles
- Skew quadrupole magnet errors (random and systematic)
- Offsets in sextupoles

Observables:

- Distortion of the tune $\delta Q_{x,y}$
- Distortion of the optics functions, e.g. beta variation
- Coupling coefficients: $g_{\pm} = \frac{1}{R} \oint \sqrt{\beta_x \beta_y} k_s(s) e^{i[\psi_x \pm \psi_y - (Q_x \pm Q_y - pN)\theta]} d\theta$

Linear coupling and correction (cont.)

Correction:

- Introduce skew quadrupole correction
- Introduce random distributions of quadrupole rolls (for simulations)
- Kick the beam at one plane and monitor tune-shift and beta distortion on the other (virtual, for simulations)
- Minimize distortions globally with skew quadrupoles
- Move working point close to coupling resonance
- Minimize optics distortion and or coupling coefficients (measured by Fourier analysis of turn-by turn BPM data)

Remarks:

- Global coupling corection with two families for each resonance
- Local coupling correction for each cell (individual powering)
- Save space with multi-function correctors (dipole + skew quadrupole + multi-pole)

Chromaticity

Linear equations of motion depend on the energy through $\delta p/p$

$$\downarrow$$

Tunes and optics functions depend on particle energy

Chromaticity:

$$\xi_{x,y} = -\frac{\Delta Q_{x,y}}{\delta p/p} \ .$$

For a linear lattice, the natural chromaticity:

$$\xi_{x,y,N} = -\frac{1}{4\pi} \oint \beta_{x,y}(s) K(s) ds \ ,$$

Chromaticity control

- Large momentum spread $\longrightarrow$ large chromatic tune-shift $\longrightarrow$ resonance crossing
- Instability compensation (Landau dumping)

Off momentum orbit on a sextupole $\longrightarrow$ quadrupole effect $\longrightarrow$ sextupole induced chromaticity:

$$\xi_{x,y,S} = -\frac{1}{2\pi} \oint \beta_{x,y}(s) b_2(s) \eta_x(s) ds \ ,$$

Correction method:

- Introduce sextupoles in high beta/dispersion areas
- Change their strength so as to acheive the desired chromaticity

Chromaticity control (cont.)

Two families of sextupoles are sufficient to control the horizontal and vertical chromaticity, at first order

Problems:

- Sextupoles introduce a beta/dispersion wave
- Second order chromaticity is not corrected

Solutions:

- Place them accordingly to cancel the effect (limited flexibility)
- Use 4 families of sextupoles

Chromaticity (cont.)

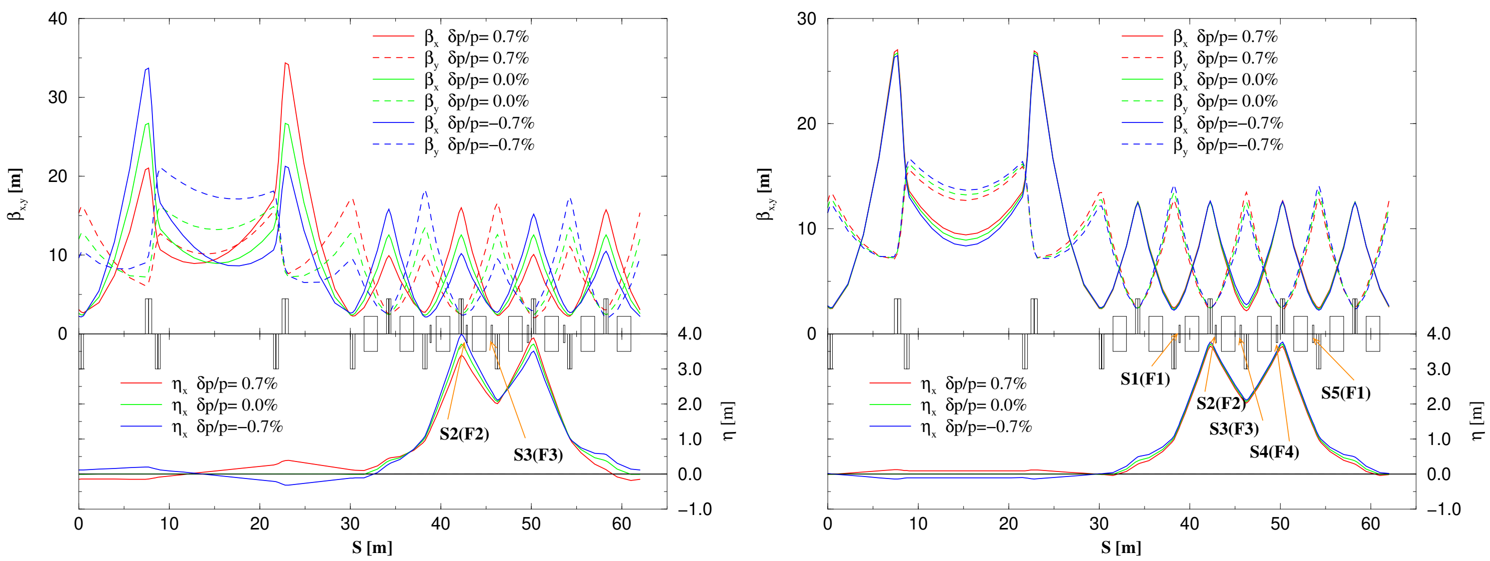

Figure 3: Lattice functions of a ring lattice using two (left) and four (right) families of sextupoles.

Chromaticity (cont.)

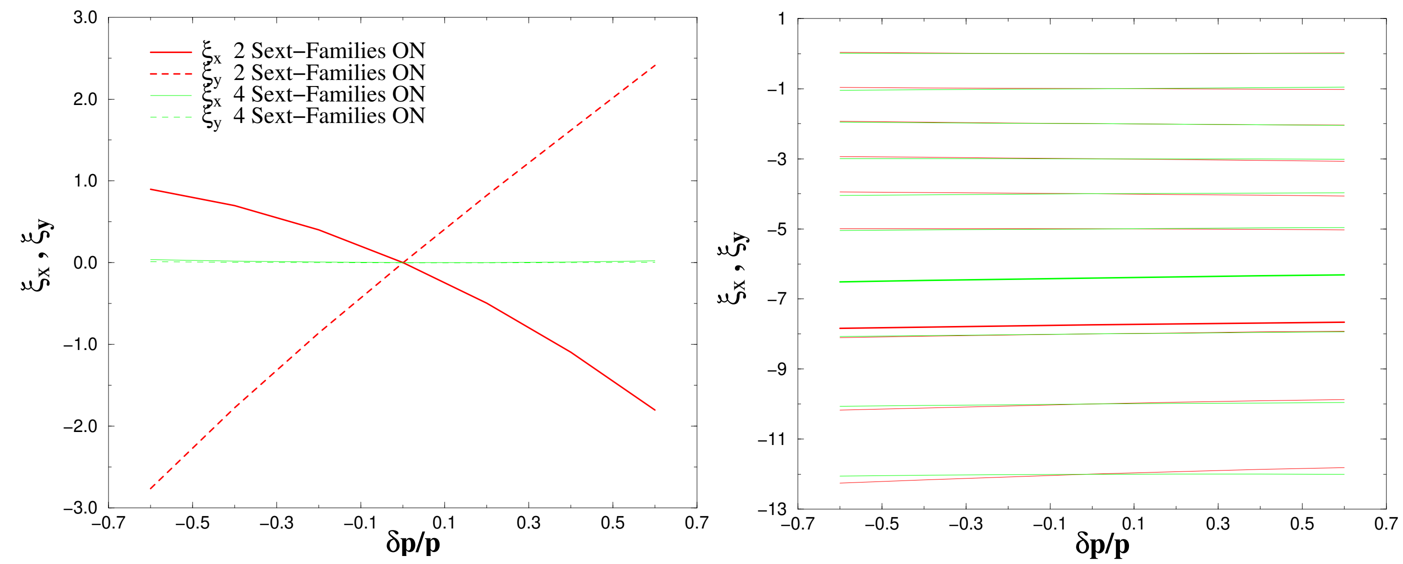

Figure 4: Plot of the chromaticities $\xi_{x,y,T}$ as a function of momentum spread, when four families of sextupoles are used. The natural chromaticities are also plotted (distinct red and green lines in the middle of the plot. This plot reflects the successful minimization of the first and second order chromatic terms, accomplished by the four sextupoles families' scheme.

Non-linear effects

- Kinematic effect
- Fringe-fields
- Magnet imperfections

Kinematic effect

Kinematic non-linearity $\rightarrow$ high-order momentum terms in the expansion of the relativistic Hamiltonian

- Negligible in high energy colliders
- Noticeable in low-energy high-intensity rings

First-order tune-shift:

$$\delta Q_{x,y} = \frac{1}{2\pi}\sum_{k=2}^{\infty}\frac{(2k-3)!!}{2^k(2k)!!}\times\sum_{\lambda=0}^{k}\lambda\binom{2\lambda}{\lambda}\binom{k}{\lambda}\binom{2(k-\lambda)}{k-\lambda}J_{x,y}^{\lambda-1}J_{y,x}^{k-\lambda}G_{x,y}$$

where $G_{x,y} = \oint_{\mathrm{ring}}\gamma_{x,y}^{\lambda}\gamma_{y,x}^{k-\lambda}ds$

Leading order $\longrightarrow$ octupole-type tune-shift

Magnet fringe-field - General field expansion

Up to now, considered only transverse field $\rightarrow$ valid for high-energy colliders but not for low-energy high-intensity rings

Fringe-field $\longrightarrow$ longitudinal dependence of magnetic field, in magnet edges Consider general 3D-field:

$$\mathbf{B}(x,y,z) = \nabla\Phi(x,y,z) = \frac{\partial\Phi}{\partial x}\mathbf{x} + \frac{\partial\Phi}{\partial y}\mathbf{y} + \frac{\partial\Phi}{\partial z}\mathbf{z} \ ,$$

where

$$\nabla^2\Phi(x,y,z) = \frac{\partial^2\Phi}{\partial x^2} + \frac{\partial^2\Phi}{\partial y^2} + \frac{\partial^2\Phi}{\partial z^2} = 0 \ .$$

Appropriate expansion:

$$\Phi(x,y,z) = \sum_{m=0}^{\infty}\sum_{n=0}^{\infty} \mathcal{C}_{m,n}(z)\frac{x^n\, y^m}{n!\, m!} \ ,$$

By Laplace equation: $\mathcal{C}_{m+2,n} = -\mathcal{C}_{m,n+2} - \mathcal{C}^{[2]}_{m,n}$

General field expansion (cont.)

The field components:

$$\begin{aligned} B_x(x,y,z) &= \sum_{m=0}^{\infty}\sum_{n=0}^{\infty}\mathcal{C}_{m,n+1}(z)\frac{x^n\,y^m}{n!\,m!} \\ B_y(x,y,z) &= \sum_{m=0}^{\infty}\sum_{n=0}^{\infty}\mathcal{C}_{m+1,n}(z)\frac{x^n\,y^m}{n!\,m!} \quad , \\ B_z(x,y,z) &= \sum_{m=0}^{\infty}\sum_{n=0}^{\infty}\mathcal{C}^{[1]}_{m,n}(z)\frac{x^n\,y^m}{n!\,m!} \end{aligned}$$

The usual normal and skew multipole coefficients are:

$$\begin{aligned} b_n(z) =& \mathcal{C}_{1,n}(z) = \left(\frac{\partial^n B_y}{\partial x^n}\right)(0,0,z) \\ a_n(z) =& \mathcal{C}_{0,n+1}(z) = \left(\frac{\partial^n B_x}{\partial x^n}\right)(0,0,z) \quad . \end{aligned}$$

Note that $\mathcal{C}_{m,n} = \sum_{l=0}^{k}(-1)^k\binom{k}{l}\mathcal{C}^{[2l]}_{m-2k,n+2k-2l}$

General field expansion (cont.)

Consider two cases, for $m = 2k$ (even) or $m = 2k+1$ (odd)

$$\mathcal{C}_{2k,n} = \sum_{l=0}^{k} (-1)^k \binom{k}{l} a^{[2l]}_{n+2k-2l-1} \ , \text{ for } n+2k-2l-1 \geq 0$$
$$\mathcal{C}_{2k+1,n} = \sum_{l=0}^{k} (-1)^k \binom{k}{l} b^{[2l]}_{n+2k-2l} \ ,$$

and finally the field components are

$$B_x(x,y,z) = \sum_{n=0}^{\infty}\sum_{m=0}^{\infty}\sum_{l=0}^{m} (-1)^m \binom{m}{l} \frac{x^n\, y^{2m}}{n!\,(2m)!} \left(b^{[2l]}_{n+2m+1-2l} \frac{y}{2m+1} + a^{[2l]}_{n+2m-2l} \right)$$
$$B_y(x,y,z) = \sum_{n=0}^{\infty}\sum_{m=0}^{\infty} (-1)^m \frac{x^n\, y^{2m}}{n!\,(2m)!} \left[\sum_{l=0}^{m} \binom{m}{l} b^{[2l]}_{n+2m-2l} - \sum_{l=0}^{m+1} \binom{m+1}{l} a^{[2l]}_{n+2m+1-2l} \frac{y}{2m+1} \right] \ ,$$
$$B_z(x,y,z) = \sum_{n=0}^{\infty}\sum_{m=0}^{\infty}\sum_{l=0}^{m} (-1)^m \binom{m}{l} \frac{x^n\, y^{2m}}{n!\,(2m)!} \left(b^{[2l+1]}_{n+2m-2l} \frac{y}{2m+1} + a^{[2l+1]}_{n+2m-1-2l} \right)$$

Approaches to study fringe-fields

1) Get an accurate magnet model

2a) Integrate equations of motion

2b) Construct a non-linear map

i) Hard-edge approximation (fringe-field length to zero)

ii) Exact integration of the magnetic field

iii) Parameter fit using "Enge" function

2c) Use your favorite non-linear dynamics tools to analyze the effect

Dipole fringe-field

Using the general z-dependent field expansion, for a straight dipole:

$$B_x = \sum_{m,n=0}^{\infty} \sum_{l=0}^{m} \frac{(-1)^m x^{2n+1} y^{2m+1}}{(2n+1)!(2m+1)!} \binom{m}{l} b_{2n+2m+2-2l}^{[2l]}$$

$$B_y = \sum_{m,n=0}^{\infty} \sum_{l=0}^{m} \frac{(-1)^m x^{2n} y^{2m}}{(2n)!(2m)!} \binom{m}{l} b_{2n+2m-2l}^{[2l]}$$

$$B_z = \sum_{m,n=0}^{\infty} \sum_{l=0}^{m} \frac{(-1)^m x^{2n} y^{2m+1}}{(2n)!(2m+1)!} \binom{m}{l} b_{2n+2m-2l}^{[2l+1]}$$

and to leading order:

$$\begin{aligned} B_x &= b_2 xy + O(4) \\ B_y &= b_0 - \frac{1}{2} b_0^{[2]} y^2 + \frac{1}{2} b_2 (x^2 - y^2) + O(4) \\ B_z &= y\ b_0^{[1]} + O(3) \end{aligned}$$

Dipole fringe to leading order gives a sextupole-like effect (vertical chromaticity)

Quadrupole fringe-field

General field expansion for a quadrupole magnet:

$$B_x = \sum_{m,n=0}^{\infty} \sum_{l=0}^{m} \frac{(-1)^m x^{2n} y^{2m+1}}{(2n)!(2m+1)!} \binom{m}{l} b_{2n+2m+1-2l}^{[2l]}$$

$$B_y = \sum_{m,n=0}^{\infty} \sum_{l=0}^{m} \frac{(-1)^m x^{2n+1} y^{2m}}{(2n+1)!(2m)!} \binom{m}{l} b_{2n+2m+1-2l}^{[2l]} \quad .$$

$$B_z = \sum_{m,n=0}^{\infty} \sum_{l=0}^{m} \frac{(-1)^m x^{2n+1} y^{2m+1}}{(2n+1)!(2m+1)!} \binom{m}{l} b_{2n+2m+1-2l}^{[2l+1]}$$

and to leading order

$$\begin{aligned} B_x &= y\left[b_1 - \frac{1}{12}(3x^2+y^2)b_1^{[2]}\right] + O(5) \\ B_y &= x\left[b_1 - \frac{1}{12}(3y^2+x^2)b_1^{[2]}\right] + O(5) \\ B_z &= xyb_1^{[1]} + O(4) \end{aligned}$$

The quadrupole fringe to leading order has an octupole-like effect

Quadrupole fringe-field (cont.)

The hard-edge Hamiltonian (Forest and Milutinovic 1988)

$$H_f = \frac{\pm Q}{12B\rho(1+\frac{\delta p}{p})}(y^3 p_y - x^3 p_x + 3x^2 y p_y - 3y^2 x p_x),$$

First order tune spread for an octupole:

$$\begin{pmatrix} \delta\nu_x \\ \delta\nu_y \end{pmatrix} = \begin{pmatrix} a_{hh} & a_{hv} \\ a_{hv} & a_{vv} \end{pmatrix} \begin{pmatrix} 2J_x \\ 2J_y \end{pmatrix},$$

where the normalized anharmonicities are

$$a_{hh} = \frac{-1}{16\pi B\rho} \sum_i \pm Q_i \beta_{xi} \alpha_{xi},$$

$$a_{hv} = \frac{1}{16\pi B\rho} \sum_i \pm Q_i (\beta_{xi}\alpha_{yi} - \beta_{yi}\alpha_{xi}),$$

$$a_{vv} = \frac{1}{16\pi B\rho} \sum_i \pm Q_i \beta_{yi} \alpha_{yi}.$$

Quadrupole fringe-field (cont.)

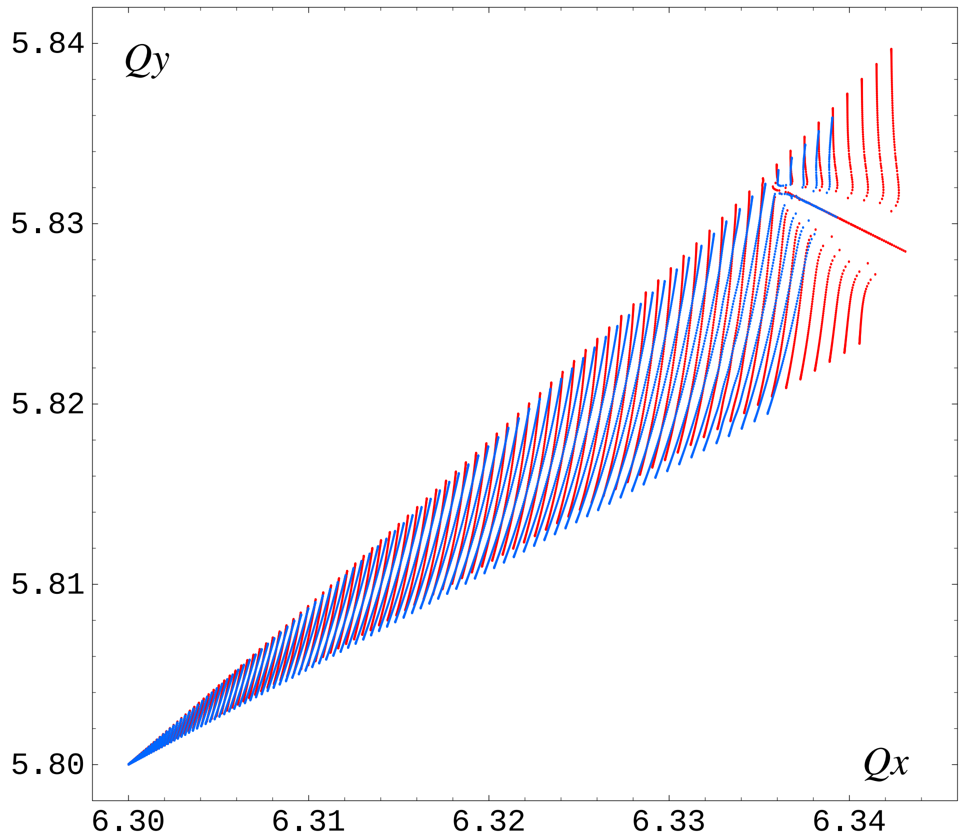

Figure 5: Tune footprints of the SNS ring, based on realistic (blue) and hard-edge (red) quadrupole fringe fields.

Multi-pole errors

A perfect $2(n+1)$-pole magnet $\rightarrow \Phi(r,\theta,z) = \Phi(r, \frac{\pi}{n+1} - \theta, z)$ which gives $n = (2j+1)(n+1) - 1$

- Normal dipole $(n = 0) \longrightarrow b_{2j}$
- Normal quadrupole $(n = 1) \longrightarrow b_{4j+1}$
- Normal sextupole $(n = 2) \longrightarrow b_{6j+2}$

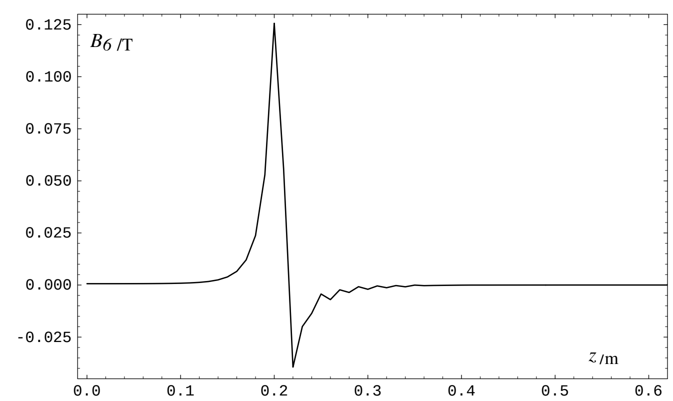

Figure 6: Dodecapole component in a 21 cm quadrupole with un-shaped ends. The reference radius is 10 cm, and the origin, $z = 0$, is at the magnet's center.

Non-linear correction

- Sextupole
- Skew-sextupole
- Octupole
- Error compensation in magnet design
- Dynamic aperture

Sextupole correction

Cause:

- Chromaticity sextupoles
- Sextupole errors in dipoles
- Dipole fringe-fields

Effect:

- Zero first order tune-spread, octupole-like second order
- Excitation of sextupole resonances $3Q_x = N$ or $Q_x \pm 2Q_y = N$

Method:

- Introduce sextupole correctors (non-dispersive areas)
- Minimize globally sextupole driving terms

Sextupole correction (cont.)

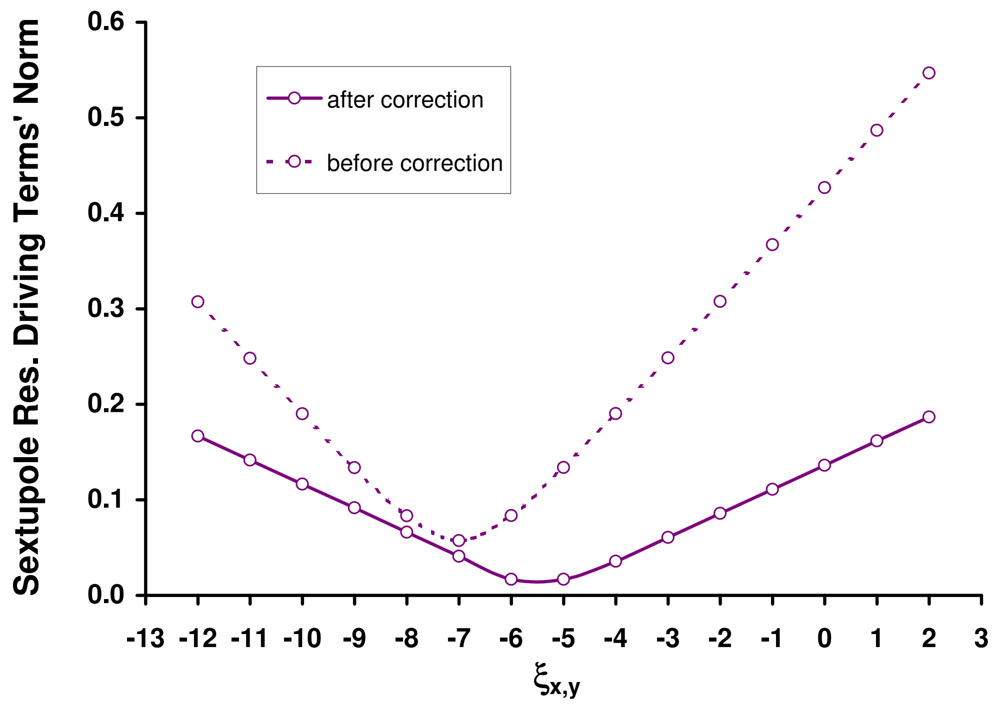

Figure 7: Norm of sextupole resonance driving terms before correction (dashed line) and after correction (solid line) with dedicated sextupole correctors. The resonance norms are reduced after the correction by as much as a factor of four.

Skew sextupole correction

Cause:

- Skew sextupole errors (dipole roll)

Effect:

- Zero first order tune-spread, octupole-like second order
- Excitation of skew sextupole resonances $3Q_y = N$ or $2Q_x \pm Q_y = N$

Method:

- Introduce skew sextupole correctors
- Tune their strength to globally minimize skew sextupole driving terms

Octupole correction

Cause:

- Quadrupole fringe-fields
- Kinematic effect
- Octupole errors in magnets
- Sextupole, skew sextupole tune-spread

Effect:

- Tune-spread linear in actions
- Excitation of normal octupole resonances $4Q_x = N$, $2Q_x \pm 2Q_y = N$ and $4Q_y = N$

Octupole correction (cont.)

Method:

- Introduce octupole correctors (in zero dispersion areas)
- Tune their strength to globally minimize tune-spread and/or driving terms

The anharmonicities become

$$A_{hh} = a_{hh} + \frac{3}{16\pi B\rho} \sum_j O_j \beta_{xj}^2,$$

$$A_{hv} = a_{hv} - \frac{6}{16\pi B\rho} \sum_j O_j \beta_{xj} \beta_{yj},$$

$$A_{vv} = a_{vv} + \frac{3}{16\pi B\rho} \sum_j O_j \beta_{yj}^2.$$

Octupole correction (cont.)

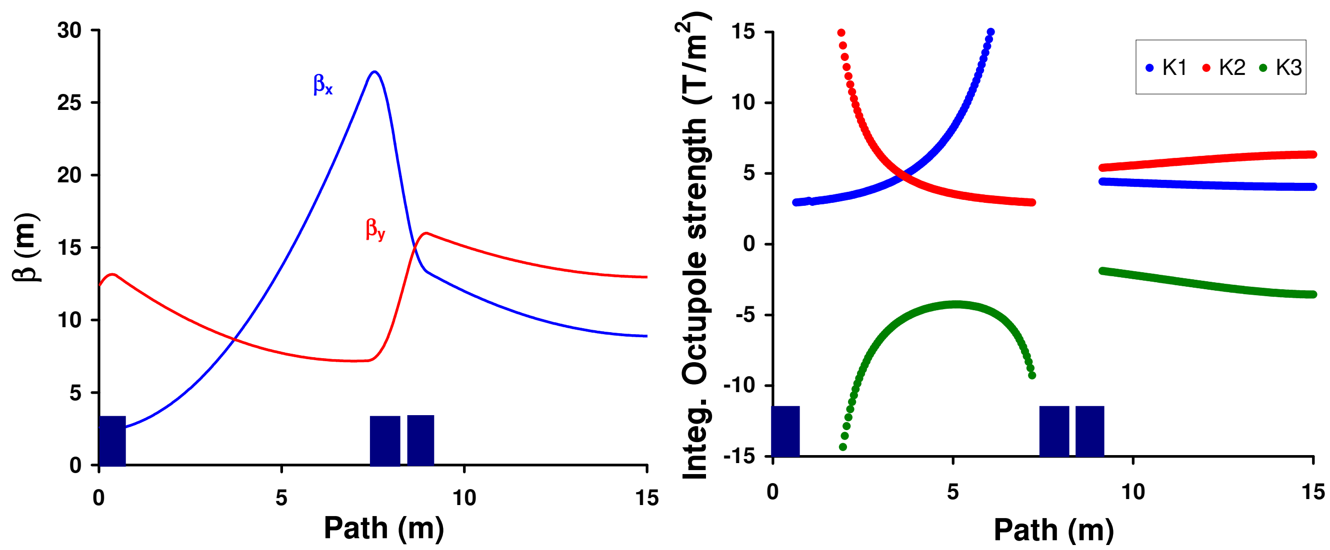

Figure 8: Top: the β functions in the first half of the SNS straight section. x Bottom: integrated strengths of three families of octupoles versus location of the third family.

Error compensation in magnet design

Example: dodecapole in quadrupoles

Tune-spread:

$$\begin{pmatrix} \delta\nu_x \\ \delta\nu_y \end{pmatrix} = \sum_i \frac{b_{5i} Q_i}{8\pi B\rho} \mathcal{D}_i \begin{pmatrix} J_x^2 \\ J_x J_y \\ J_y^2 \end{pmatrix},$$

where $\mathcal{D}_i$ denotes the 3×2 matrix

$$\begin{pmatrix} \beta_{xi}^3 & -6\beta_{xi}^2\beta_{yi} & 3\beta_{xi}\beta_{yi}^2 \\ -3\beta_{xi}^2\beta_{yi} & 6\beta_{xi}\beta_{yi}^2 & -\beta_{yi}^3 \end{pmatrix}.$$

i.e. quadratic in the actions.

Method of correction $\longrightarrow$ Shape ends of the quadrupoles (local correction)

Error compensation in magnet design (cont.)

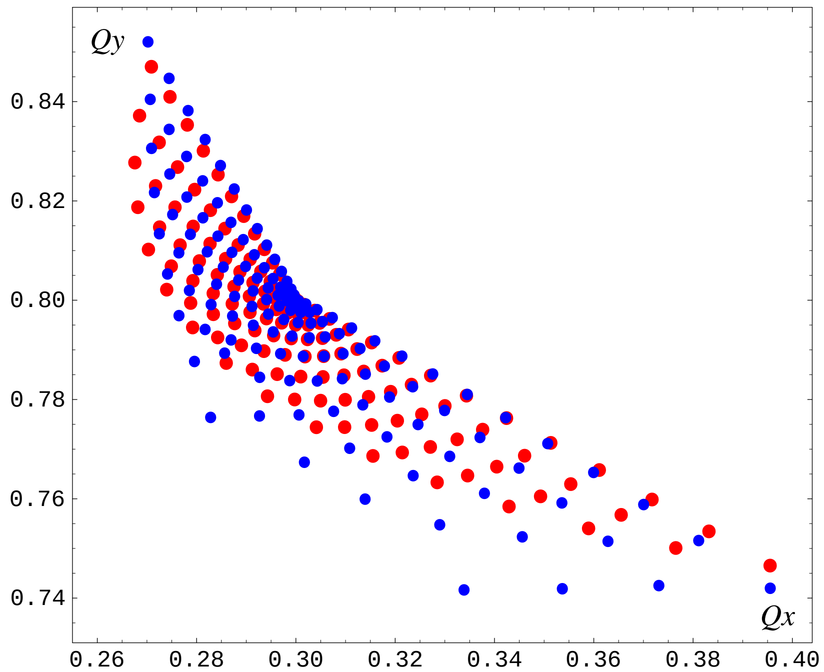

Figure 9: Tune footprints of a ring lattice with a dodecapole error in the quadrupoles of $b_5 = 60$ units; results are from tracking data (blue) or the analytic estimate (red).

Error compensation in magnet design (cont.)

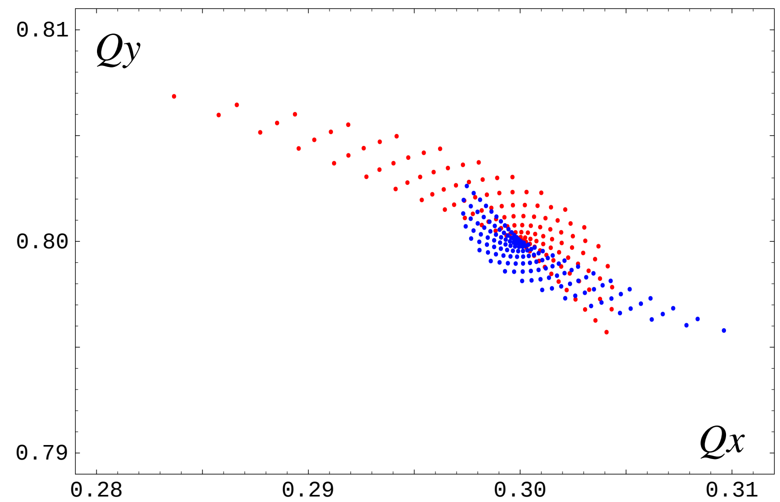

Figure 10: Comparison of tune-shift plots using body (red) and local (blue) compensation of the dodecapole component in the SNS ring quadrupoles.

Dynamic aperture)

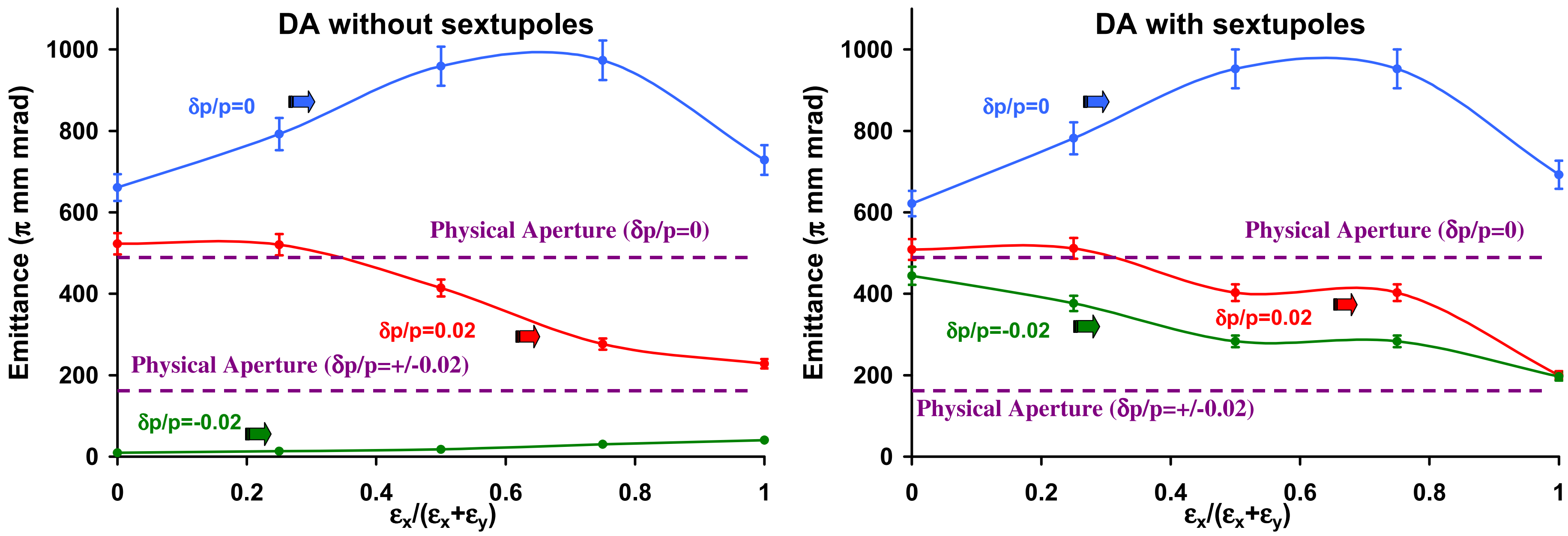

Figure 11: Dynamic aperture for the working point (6.3,5.8), without (left) and with (right) sextupoles.

Scaling law for magnet fringe-field

Field of a streight **dipole** magnet at leading order:

$$\begin{aligned} B_x &= b_2 xy + O(4) \\ B_y &= b_0 - \frac{1}{2} b_0^{[2]} y^2 + \frac{1}{2} b_2 (x^2 - y^2) + O(4) \\ B_z &= y\, b_0^{[1]} + O(3) \end{aligned}$$

The change of transverse momentum imparted by the dipole field is:

$$\Delta p^b = -e \int_{\text{body}} v_z b_0 dz \approx -e v_z \overline{b_0} L_{\text{eff}}$$

with $L_{\text{eff}} = \int_{\text{body}} b_0 dz / \overline{b_0}$ the effective length and $\overline{b_0}$ the main dipole field.

Scaling law for magnet fringe-field (cont.)

The momentum kick imparted by the fringe field:

$$\Delta p^f_{x,y} = \Delta p^f_{x,y}(\|) + \Delta p^f_{x,y}(\perp) \quad ,$$

where

$$\begin{aligned} \Delta p^f_x(\|) &= \quad e \int_{\text{fringe}} v_z y' B_z(x,y,z) dz \\ \Delta p^f_y(\|) &= - \quad e \int_{\text{fringe}} v_z x' B_z(x,y,z) dz \end{aligned} \quad ,$$

the momentum increments caused by the longitudinal component of the magnetic field and

$$\begin{aligned} \Delta p^f_x(\perp) &= - \quad e \int_{\text{fringe}} v_z B_y(x,y,z) dz \\ \Delta p^f_y(\perp) &= \quad e \int_{\text{fringe}} v_z B_x(x,y,z) dz \end{aligned} \quad ,$$

the momentum increments by the transverse components of the magnetic field.

Scaling law for magnet fringe-field (cont.)

The momentum increments of the particle caused by the longitudinal component:

$$\Delta p_x^f(\|) = e \int_{\text{fringe}} v_z y' B_z dz \approx e v_z \overline{b_0} y y' \ , \qquad \Delta p_y^f(\|) = -e \int_{\text{fringe}} v_z x' B_z dz \approx -e v_z \overline{b_0} y x' \ .$$

The momentum increments caused by the transverse component of the dipole fringe fields are:

$$\Delta p_x^f(\perp) = -e \int v_z B_y dz \approx e v_z \overline{b_0} y y' \ , \qquad \Delta p_y^f(\perp) = e \int v_z B_x dz \approx 0 \ .$$

The total momentum increments:

$$\Delta p_x^f \approx 2 e v_z \overline{b_0} y y' \ , \qquad \Delta p_y^f \approx -e v_z \overline{b_0} y x' \ .$$

Scaling law for magnet fringe-field (cont.)

The total rms transverse momentum kick by the fringe field:

$$(\Delta p_\perp^f)_{rms} = \sqrt{\langle(\Delta p_x^f)^2\rangle + \langle(\Delta p_y^f)^2\rangle} = e v_z \overline{b_0}\sqrt{4\langle y^2 y'^2\rangle + \langle y^2 x'^2\rangle} \quad ,$$

where $\langle . \rangle$ denotes the average over the angle variables and

$$\langle y^2 y'^2\rangle = \frac{(1+3\alpha_y)\epsilon_y^2}{8} \quad , \qquad \langle y^2 x'^2\rangle = \langle y^2\rangle\langle x'^2\rangle = \frac{(1+\alpha_x)\beta_y\epsilon_x\epsilon_y}{4\beta_x} \quad .$$

The rms transverse momentum kick becomes

$$(\Delta p_\perp^f)_{rms} = e v_z \overline{b_0}\sqrt{\frac{(1+3\alpha_y)\epsilon_y^2}{8} + \frac{(1+\alpha_x)\beta_y\epsilon_x\epsilon_y}{4\beta_x}} \quad ,$$

Scaling law for magnet fringe-field (cont.)

Ratio between momentum increment produced by dipole fringe field to the dipole body

$$\frac{(\Delta p^f_\perp)_{rms}}{(\Delta p^b_\perp)_{rms}} \approx \frac{1}{L_{\rm eff}}\sqrt{\frac{(1+3\alpha_y)\epsilon_y^2}{8}+\frac{(1+\alpha_x)\beta_y\epsilon_x\epsilon_y}{4\beta_x}} \quad .$$

If α small:

$$\frac{(\Delta p^f_\perp)_{rms}}{(\Delta p^b_\perp)_{rms}} \approx \frac{\epsilon_\perp}{L_{\rm eff}} \quad ,$$

where $\epsilon_\perp$ the rms beam transverse emittance.

When α or α_y large:

$$\frac{(\Delta p^f_\perp)_{rms}}{(\Delta p^b_\perp)_{rms}} \approx \alpha\frac{\epsilon_\perp}{L_{\rm eff}} \quad ,$$

where α the maximum of α_x or α_y.

Scaling law for magnet fringe-field (cont.)

The quadrupole magnetic field in leading order:

$$
\begin{aligned}
B_x &= y\left[b_1 - \frac{1}{12}(3x^2+y^2)b_1^{[2]}\right] + O(5) \\
B_y &= x\left[b_1 - \frac{1}{12}(3y^2+x^2)b_1^{[2]}\right] + O(5) \\
B_z &= xyb_1^{[1]} + O(4)
\end{aligned}
$$

where $b_1(z)$ the transverse field gradient. The momentum increments for body part

$$\Delta p_x^b = -ev_z\overline{b_1}xL_{\text{eff}} \ , \qquad \Delta p_y^b = ev_z\overline{b_1}yL_{\text{eff}} \ ,$$

where $L_{\text{eff}} = \int_{\text{body}} b_1 dz/\overline{b_1}$ is the effective length.

Scaling law for magnet fringe-field (cont.)

The momentum increments from the longitudinal field component

$$\Delta p_x^f(\|) \approx e v_z x y y' \overline{b_1} \quad , \qquad \Delta p_y^f(\|) \approx -e v_z x y x' \overline{b_1} \quad ,$$

and the momentum increment by the transverse component of the fringe fields

$$\Delta p_x^f(\perp) \approx \frac{-e v_z \overline{b_1}}{4}\left[2xyy' + (x^2+y^2)x'\right] \quad , \qquad \Delta p_y^f(\perp) \approx \frac{e v_z \overline{b_1}}{4}\left[2xx'y + (x^2+y^2)y'\right] \quad .$$

Combining the contributions

$$\begin{aligned} \Delta p_x^f &\approx \frac{e v_z \overline{b_1}}{4}\left[2xyy' - (x^2+y^2)x'\right] \\ \Delta p_y^f &\approx \frac{e v_z \overline{b_1}}{4}\left[-2xx'y + (x^2+y^2)y'\right] \end{aligned} \quad .$$

Scaling law for magnet fringe-field (cont.)

The total rms transverse momentum kick

$$(\Delta p_\perp^f)_{rms} \approx \frac{ev_z\overline{b_1}}{16} \left\{ (1+5\alpha_x)\beta_x\epsilon_x^3 + \frac{3}{\beta_y}\left[(1+\alpha_y)\beta_x^2 - 8\alpha_x\alpha_y\beta_x\beta_y + 2(1+3\alpha_x)\beta_y^2\right]\epsilon_x^2\epsilon_y \right. \\ \left. +(1+5\alpha_y)\beta_y\epsilon_y^3 + \frac{3}{\beta_x}\left[(1+\alpha_x)\beta_y^2 - 8\alpha_x\alpha_y\beta_x\beta_y + 2(1+3\alpha_y)\beta_x^2\right]\epsilon_x\epsilon_y^2 \right\}^{1/2},$$

Ratio between momentum increment from fringe field to that of the body

$$(\Delta p_\perp^f)_{rms} \approx \frac{1}{8L_{\rm eff}}\left\{ \frac{(1+5\alpha_x)\beta_x^2\beta_y\epsilon_x^3 + 3\beta_x\left[(1+\alpha_y)\beta_x^2 - 8\alpha_x\alpha_y\beta_x\beta_y + 2(1+3\alpha_x)\beta_y^2\right]\epsilon_x^2\epsilon_y}{2\beta_x\beta_y(\overline{\beta_x}\epsilon_x + \overline{\beta_y}\epsilon_y)} \right. \\ \left. + \frac{(1+5\alpha_y)\beta_x\beta_y^2\epsilon_y^3 + 3\beta_y\left[(1+\alpha_x)\beta_y^2 - 8\alpha_x\alpha_y\beta_x\beta_y + 2(1+3\alpha_y)\beta_x^2\right]\epsilon_x\epsilon_y^2}{2\beta_x\beta_y(\overline{\beta_x}\epsilon_x + \overline{\beta_y}\epsilon_y)} \right\}^{1/2},$$

Crude estimate, for α small:

$$\frac{(\Delta p_\perp^f)_{rms}}{(\Delta p_\perp^b)_{rms}} \approx \frac{\epsilon_\perp}{L_{\rm eff}},$$

and when αs are large:

$$\frac{(\Delta p_\perp^f)_{\mathrm{r}ms}}{(\Delta p_\perp^b)_{\mathrm{r}ms}} \approx \alpha \frac{\epsilon_\perp}{L_{\mathrm{eff}}} \quad ,$$

where α is the maximum of α_x or α_y.

Scaling law for magnet fringe-field (cont.)

General multipole expansion to leading order:

$$B_x(x,y,z) = \Im m\left\{\frac{(x+iy)^n b_n(z)}{n!} - \frac{(x+iy)^{n+1}\left[(n+3)x - i(n+1)y\right] b_n^{[2]}(z)}{4(n+2)!} + O(n+4)\right\}$$

$$B_y(x,y,z) = \Re e\left\{\frac{(x+iy)^n b_n(z)}{n!} - \frac{(x+iy)^{n+1}\left[(n+1)x - i(n+3)y\right] b_n^{[2]}(z)}{4(n+2)!} + O(n+4)\right\} ,$$

$$B_z(x,y,z) = \Im m\left\{\frac{(x+iy)^{n+1} b_n^{[1]}(z)}{(n+1)!} + O(n+3)\right\}$$

The body part

$$\Delta p_x^b = - e\int_{\text{body}} v_z B_y(x,y,z)dz \approx - e v_z \overline{b_n} L_{\text{eff}} \frac{\Re e\left\{(x+iy)^n\right\}}{n!}$$

$$\Delta p_y^b = e\int_{\text{body}} v_z B_x(x,y,z)dz \approx e v_z \overline{b_n} L_{\text{eff}} \frac{\Im m\left\{(x+iy)^n\right\}}{n!}$$

where $L_{eff} = \int_{\text{body}} b_n(z)dz/\overline{b_n}$ is the effective length.

Scaling law for magnet fringe-field (cont.)

The fringe part:

$$\Delta p_x^f(\|) \approx \frac{ev_z\overline{b_n}}{(n+1)!}\Im m\left\{(x+iy)^{n+1}\right\}y'$$

$$\Delta p_y^f(\|) \approx -\frac{ev_z\overline{b_n}}{(n+1)!}\Im m\left\{(x+iy)^{n+1}\right\}x'$$

.

and

$$\Delta p_x^f(\perp) \approx \frac{-ev_z\overline{b_n}}{4(n+1)!}\Re e\left\{(x+iy)^n\left[(n+1)xx'+(n+3)yy'+i(n-1)xy'-i(n+1)yx'\right]\right\}$$

,

$$\Delta p_y^f(\perp) \approx \frac{ev_z\overline{b_n}}{4(n+1)!}\Im m\left\{(x+iy)^n\left[(n+3)xx'+(n+1)yy'+i(n+1)xy'-i(n-1)yx'\right]\right\}$$

The total momentum increments:

$$\Delta p_x^f \approx -\frac{ev_z\overline{b_n}}{4(n+1)!}\Re e\left\{(x+iy)^n\left[(n+1)(x-iy)(x'+iy')+2iy'(x+iy)\right]\right\}$$

.

$$\Delta p_y^f \approx \frac{ev_z\overline{b_n}}{4(n+1)!}\Im m\left\{(x+iy)^n\left[(n+1)(x-iy)(x'+iy')-2x'(x+iy)\right]\right\}$$

Scaling law for magnet fringe-field (cont.)

$$(\Delta p_\perp^f)_{rms} \approx \frac{ev_z\overline{b_n}}{2^{n+3}(n+1)!}\left[\sum_{l=0}^{n}\binom{2(n-l)}{n-l}\binom{2l}{l}\beta_x^{n-l}\beta_y^l\epsilon_x^{n-l}\epsilon_y^l\sum_{m=0}^{2}g_{n,l,m}(\alpha_{x,y},\beta_{x,y})\epsilon_x^m\epsilon_y^{2-m}\right]^{1/2},$$

$$(\Delta p_\perp^b)_{rms} \approx \frac{ev_z\overline{b_n}L_{\rm eff}}{2^n n!}\left[\sum_{l=0}^{n}\binom{n}{l}\binom{2(n-l)}{n-l}\binom{2l}{l}\overline{\beta_x^{n-l}\beta_y^l}\epsilon_x^{n-l}\epsilon_y^l\right]^{1/2}$$

The coefficients

$$g_{n,l,0}(\alpha_{x,y},\beta_{x,y}) = \frac{\left[(n^2+1)(2l+1)\binom{n}{l} - 2l(2n+1)(-1)^l\binom{2n}{2l}\right][1+(2l+3)\alpha_y]}{(l+1)(l+2)} - \frac{8(n+1)(n-l)(2l+3)(-1)^l\binom{2n}{2l}\alpha_x\alpha_y\beta_y}{\beta_x(l+1)(l+2)}$$

$$g_{n,l,1}(\alpha_{x,y},\beta_{x,y}) = \frac{\left[(n^2+4n+5)(2l+1)\binom{n}{l} + 2(5n+2ln+2)(-1)^l\binom{2n}{2l}\right][1+(2n-2l+1)\alpha_x]\beta_y}{\beta_x(n-l+1)(l+1)} + \frac{\left[(n^2+4n+5)\binom{n}{l} - 2(n+2)(-1)^l\binom{2n}{2l}\right](2n-2l+1)[1+(2l+1)\alpha_y]\beta_x}{\beta_y(n-l+1)(l+1)} - \frac{8(n+1)\left[(2l+1)\binom{n}{l} + (n-l)(-1)^l\binom{2n}{2l}\right](2n-2l+1)\alpha_x\alpha_y}{(n-l+1)(l+1)},$$

$$g_{n,l,2}(\alpha_{x,y},\beta_{x,y}) = \frac{\left[(n^2+1)\binom{n}{l} + 2n(-1)^l\binom{2n}{2l}\right](2n-2l+1)[1+(2n-2l+3)\alpha_x]}{(n-l+1)(n-l+2)}$$

Scaling law for magnet fringe-field (cont.)

For flat beam (vertical y, y' vanishes) and the total transverse rms momentum increment for the body

$$(\Delta p_\perp^b)_{rms} \equiv \sqrt{\langle(\Delta p_x^b)^2\rangle} \approx \frac{ev_z\overline{b_n}L_{\rm eff}}{2^n n!}\sqrt{\binom{2n}{n}\overline{\beta^n}\epsilon_\perp^n} \ ,$$

where $\overline{\beta^n}$ the average of β^n and $\epsilon_\perp$ the rms beam transverse emittance. For the fringe:

$$(\Delta p_\perp^f)_{rms} \equiv \sqrt{\langle(\Delta p_x^f)^2\rangle} \approx \frac{ev_z\overline{b_n}}{2^{n+3}n!}\sqrt{\binom{2n+2}{n+1}\frac{\beta^n[1+(2n+3)\alpha^2]}{2(n+2)}\epsilon_\perp^{n+2}} \ ,$$

Scaling law for magnet fringe-field (cont.)

The ratio of the rms momentum transverse kicks:

$$\frac{(\Delta p_\perp^f)_{rms}}{(\Delta p_\perp^b)_{rms}} \approx \frac{\epsilon_\perp}{8L_{\rm eff}}\sqrt{\frac{(2n+1)\beta^n[1+(2n+3)\alpha^2]}{(n+1)(n+2)\overline{\beta^n}}} \quad ,$$

Considering beta functions are not varying rapidly:

$$\frac{(\Delta p_\perp^f)_{rms}}{(\Delta p_\perp^b)_{rms}} \approx \frac{\epsilon_\perp}{L_{\rm eff}} \quad ,$$

When α anomalously large:

$$\frac{(\Delta p_\perp^f)_{rms}}{(\Delta p_\perp^b)_{rms}} \approx \alpha\frac{\epsilon_\perp}{L_{\rm eff}} \quad ,$$

Scaling law for magnet fringe-field (cont.)

For a round beam, transverse emittances are equal $\epsilon_x = \epsilon_y = \epsilon_\perp$. For simplicity, $\beta_x \approx \beta_y = \beta$ and $\alpha_x \approx \alpha_y = \alpha$ and $\overline{\beta^n} \approx \overline{\beta}^n$ and the total transverse rms momentum increment for the body:

$$(\Delta p_\perp^b)_{rms} \approx \frac{e v_z \overline{b_n} L_{\text{eff}}}{2^{n/2} n!} \overline{\beta}^{n/2} \epsilon_\perp^{n/2} \left[{}_3F_2(1/2, -n, -n; 1, 1/2 - n; 1) \frac{(2n-1)!!}{n!} \right]^{1/2} \quad ,$$

The rms momentum kick given by the fringe field is:

$$(\Delta p_\perp^f)_{rms} \approx \frac{e v_z \overline{b_n} \beta^{n/2} \epsilon_\perp^{n/2+1}}{2^{n+3}(n+1)!} \left[\sum_{l=0}^{n} \binom{2(n-l)}{n-l} \binom{2l}{l} g_{n,l}(\alpha) \right]^{1/2} \quad ,$$

Scaling law for magnet fringe-field (cont.)

The ratio of the rms momentum transverse kicks is:

$$\frac{(\Delta p_\perp^f)_{rms}}{(\Delta p_\perp^b)_{rms}} \approx \frac{\epsilon_\perp}{L_{\text{eff}}} \frac{\beta^{n/2}}{\overline{\beta}^{n/2}} C_n(\alpha) \quad ,$$

where the coefficient C_n is:

$$C_n(\alpha) = \frac{1}{8(n+1)} \left[\frac{n! \sum_{l=0}^{n} \binom{2(n-l)}{n-l} \binom{2l}{l} g_{n,l}(\alpha)}{{}_3F_2(1/2, -n, -n; 1, 1/2 - n; 1)(2n-1)!!} \right]^{1/2} \quad ,$$

For small α functions:

$$\frac{(\Delta p_\perp^f)_{rms}}{(\Delta p_\perp^b)_{rms}} \approx \frac{\epsilon_\perp}{L_{\text{eff}}} \quad ,$$

and for α large:

$$\frac{(\Delta p_\perp^f)_{rms}}{(\Delta p_\perp^b)_{rms}} \approx \alpha \frac{\epsilon_\perp}{L_{\text{eff}}} \quad ,$$

Frequency Maps

Perturbation theory $\longrightarrow$ insight about non-linear

Problem: Construction of normal forms or action variables cannot be applied for large perturbations

Need a method to represent the systems' global dynamics

$$\downarrow$$

Frequency map analysis (Laskar 1988, 1990)

Algorithm to precisely compute frequencies associated with KAM tori of tracked orbits

Frequency Maps (cont.)

NAFF algorithm $\longrightarrow$ quasi-periodic approximation, truncated to order N,

$$f'_j(t) = \sum_{k=1}^{N} a_{j,k} e^{i\omega_{jk} t} \ ,$$

with $f'_j(t), a_{j,k} \in \mathbb{C}$ and $j = 1, \ldots, n$, of a complex function $f_j(t) = q_j(t) + ip_j(t)$, formed by a pair of conjugate variables determined by usual numerical integration, for a finite time span $t = \tau$.

Recover the frequency vector $\boldsymbol{\nu} = (\nu_1, \nu_2, \ldots, \nu_n) \longrightarrow$ parameterizes KAM tori.

Frequency Maps (cont.)

Construct frequency map by repeating procedure for set of initial conditions.

Example: Keep all the $\boldsymbol{q}$ variables constant, and explore the momenta $\boldsymbol{p}$ to produce the map $\mathcal{F}_\tau$:

$$\mathcal{F}_\tau \;:\; \begin{array}{ccc} \mathbb{R}^n & \longrightarrow & \mathbb{R}^n \\ \boldsymbol{p}|_{\boldsymbol{q}=\boldsymbol{q}_0} & \longrightarrow & \boldsymbol{\nu} \;. \end{array}$$

Dynamics of the system analyzed by studying the regularity of the frequency map.

Frequency Maps (cont.)

F.M.A is applied to tracking data N,

$$f_j'(t) = \sum_{k=1}^{N} a_{j,k} e^{i\omega_{jk} t} \ ,$$

with $f_j'(t), a_{j,k} \in \mathbb{C}$ and $j = 1, \ldots, n$, of a complex function $f_j(t) = q_j(t) + ip_j(t)$, formed by a pair of conjugate variables determined by usual numerical integration, for a finite time span $t = \tau$.

Recover the frequency vector $\boldsymbol{\nu} = (\nu_1, \nu_2, \ldots, \nu_n) \longrightarrow$ parameterizes KAM tori.

Frequency Maps (cont.)

Construct frequency map by repeating procedure for set of initial conditions.

Example: Keep all the $\boldsymbol{q}$ variables constant, and explore the momenta $\boldsymbol{p}$ to produce the map $\mathcal{F}_\tau$:

$$\mathcal{F}_\tau \; : \; \begin{array}{ccc} \mathbb{R}^n & \longrightarrow & \mathbb{R}^n \\ \boldsymbol{p}|_{\boldsymbol{q}=\boldsymbol{q}_0} & \longrightarrow & \boldsymbol{\nu} \; . \end{array}$$

Dynamics of the system analyzed by studying the regularity of the frequency map.

Frequency Maps (cont.)

F.M.A is applied to tracking data ($\tau = 500$ turns), for large number of initial conditions ($\approx 10^4$).

Particle coordinates distributed uniformly on Courant-Snyder invariants A_{x0} and A_{y0}, at different ratios A_{x0}/A_{y0}.

The map is

$$\mathcal{F}_\tau \ : \ \begin{array}{ccc} \mathbb{R}^2 & \longrightarrow & \mathbb{R}^2 \\ (I_x, I_y)|_{p_x, p_y = 0}, & \longrightarrow & (\nu_x, \nu_y) \end{array},$$

Frequency Maps (cont.)

Example:

Frequency maps for working point (6.3,5.8) of SNS accumulator ring.

- Inject $\tilde{1}000$ particles with different amplitudes up to a
- Maximum emittance of 480 π mm mrad
- Five different momentum spreads ($\delta p/p = 0, \pm 0.1, \pm 0.15$)
- Small magnet field errors ($10^{-}-4$ level)
- Quadrupole fringe fields in the "hard-edge" approximation

Frequency Maps (cont.)

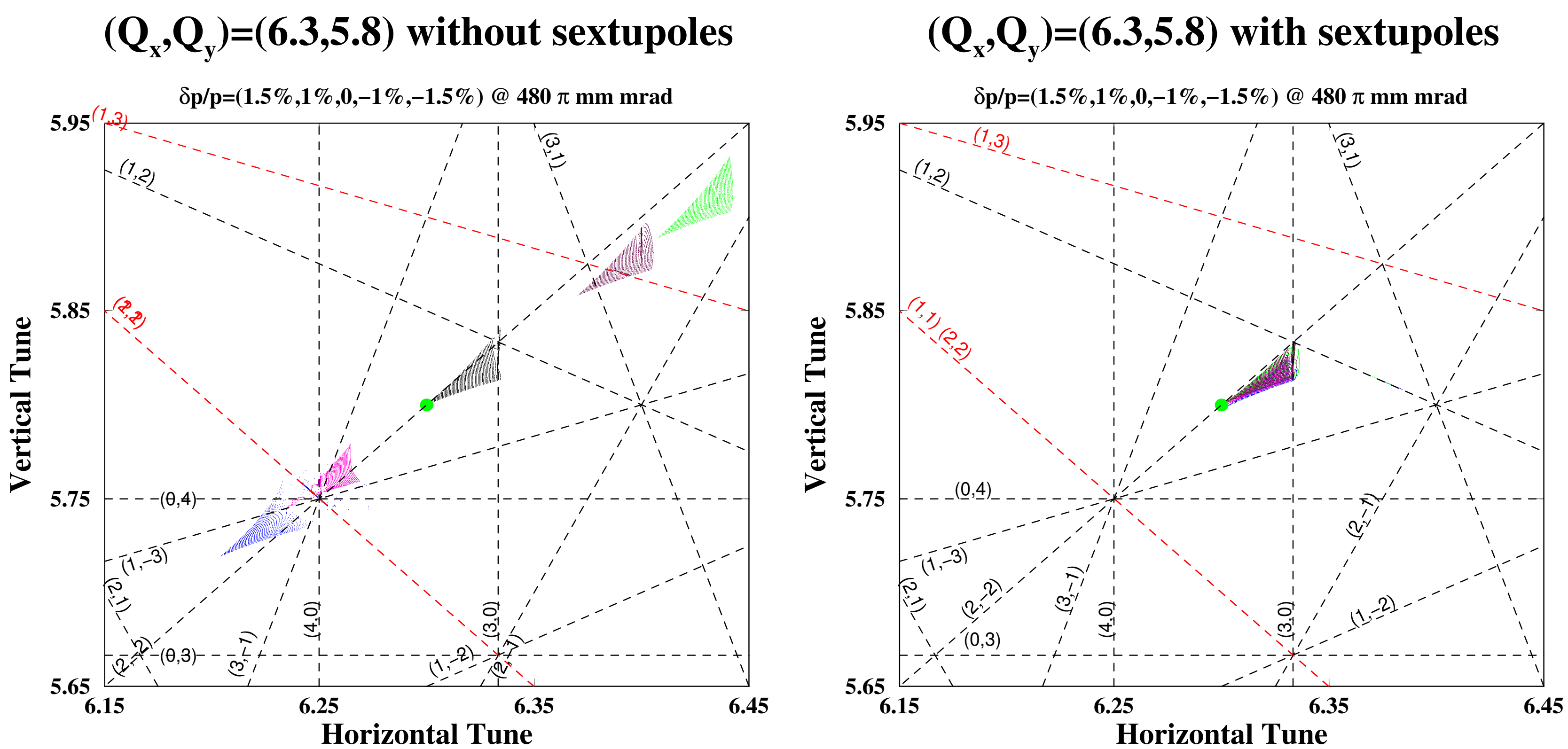

Figure 12: Frequency maps for the working point (6.3,5.8), without (left) and with (right) sextupoles.

Frequency Maps (cont.)

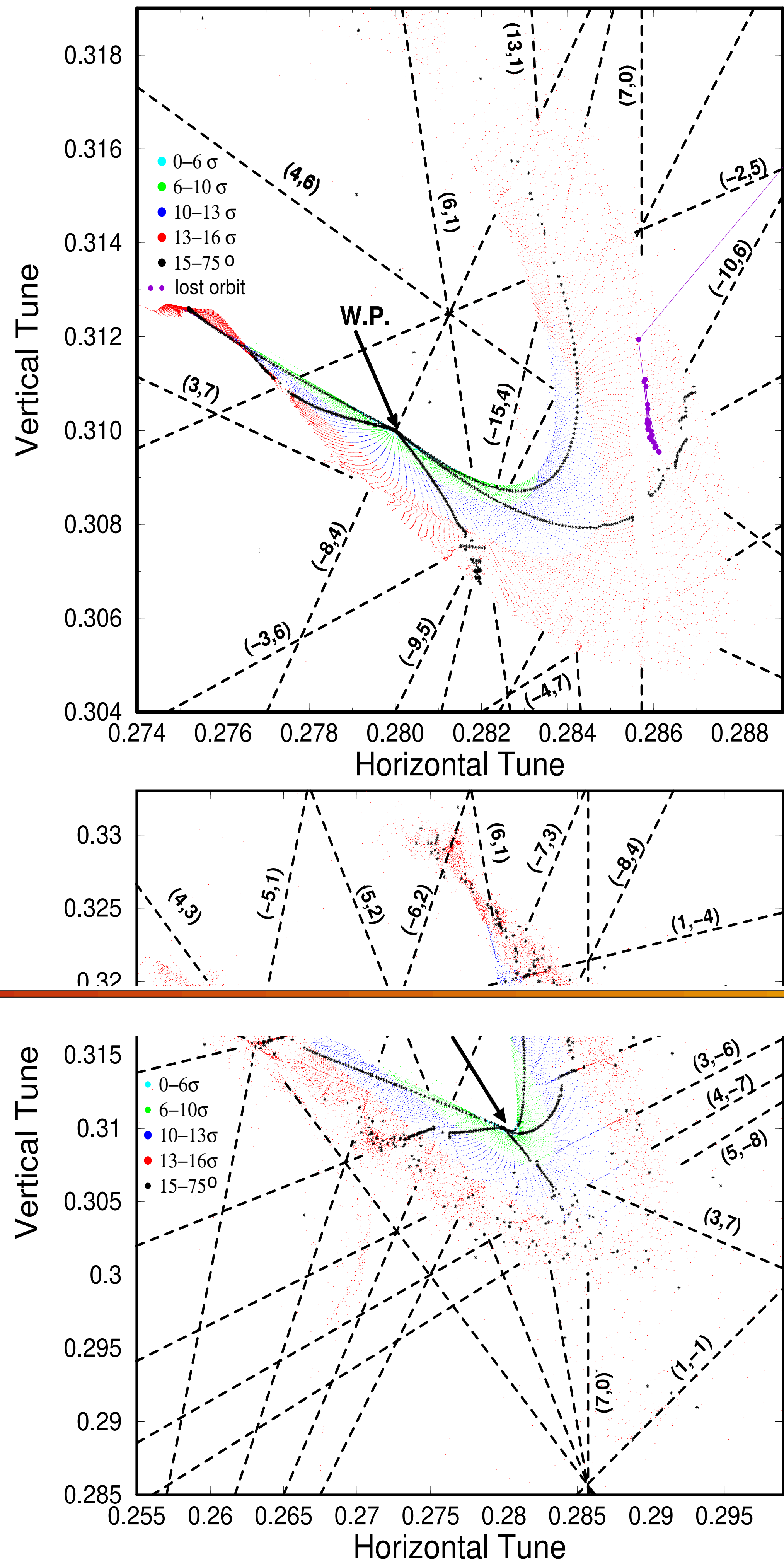

Figure 13: Frequency maps for the LHC

Diffusion Maps

Calculate tune for two equal and successive time spans and compute diffusion vector:

$$\boldsymbol{D}|_{t=\tau} = \boldsymbol{\nu}|_{t\in(0,\tau/2]} - \boldsymbol{\nu}|_{t\in(\tau/2,\tau]} \ ,$$

Plot the points in (A_{x0}, A_{y0})–space with a different colors

- grey for stable ($|\boldsymbol{D}| \leq 10^{-7}$) to
- black for strongly chaotic particles ($|\boldsymbol{D}| > 10^{-2}$).

Diffusion quality factor:

$$D_{QF} = \left\langle \frac{|\boldsymbol{D}|}{(I_{x0}^2 + I_{y0}^2)^{1/2}} \right\rangle_R \ .$$

Diffusion Maps (cont.)

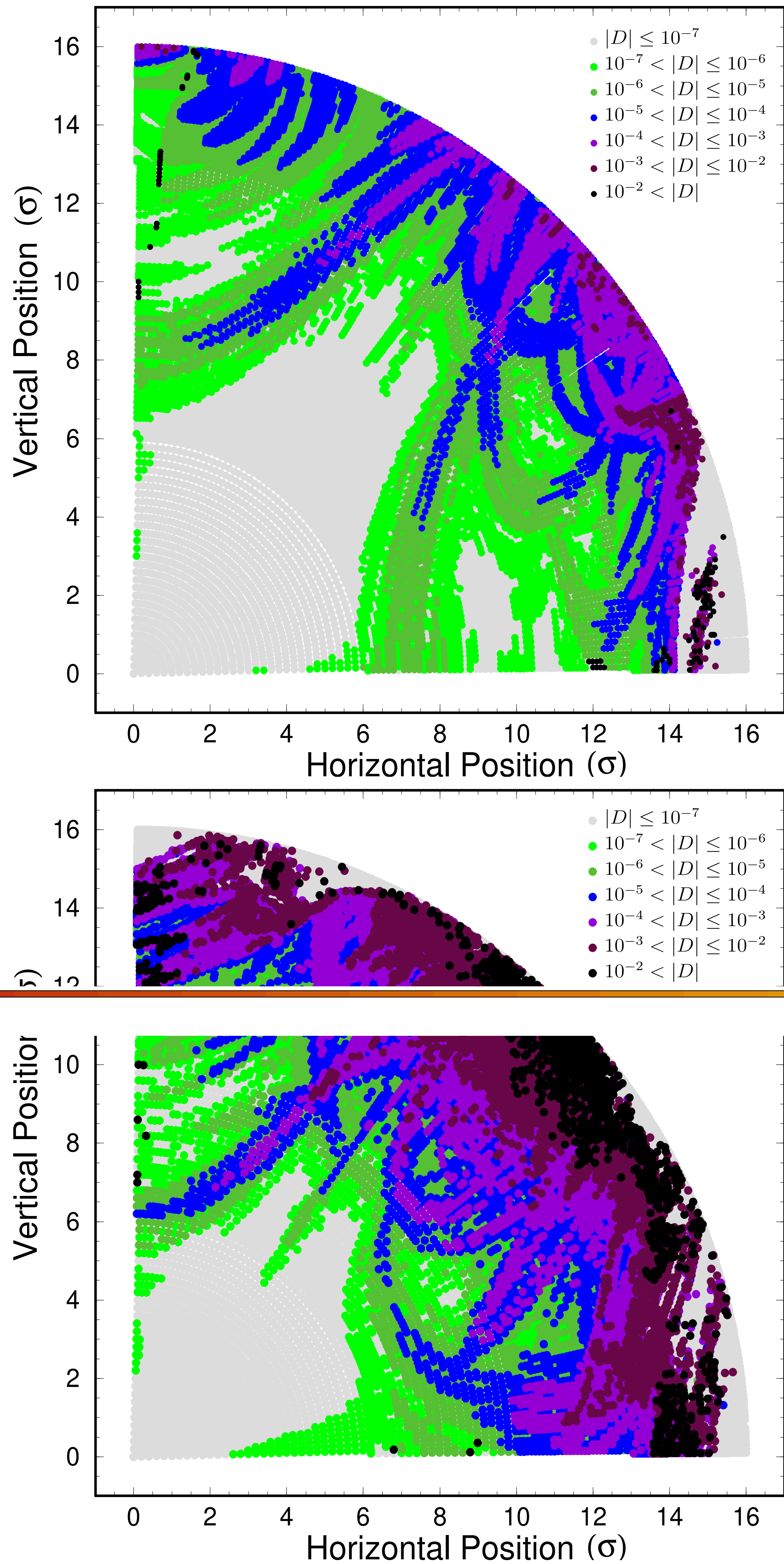

Figure 14: Diffusion maps